Title	A comparative study of wavelength-dependent photoinactivation in photosystem II of drought-tolerant photosynthetic organisms in Antarctica and the potential risks of photoinhibition in the habitat
Authors	Kosugi Makiko, Maruo Fumino, Inoue Takeshi, Kurosawa Norio, Kawamata Akinori, Koike Hiroyuki, Kamei Yasuhiro, Kudoh Sakae, Imura Satoshi
Citation	Annals of Botany, 122(7), 1263-1278, 2018
Issue Date	2018-7-23
Type	Journal Article
URL	https://doi.org/10.1093/aob/mcy139
Right	
Textversion	publisher

Annals of Botany **122**: 1263–1278, 2018
doi: 10.1093/aob/mcy139, available online at www.academic.oup.com/aob

ANNALS OF BOTANY
Founded 1887

A comparative study of wavelength-dependent photoinactivation in photosystem II of drought-tolerant photosynthetic organisms in Antarctica and the potential risks of photoinhibition in the habitat

Makiko Kosugi[1,2,*], Fumino Maruo[3], Takeshi Inoue[3], Norio Kurosawa[4], Akinori Kawamata[5], Hiroyuki Koike[2], Yasuhiro Kamei[6,7], Sakae Kudoh[1,3] and Satoshi Imura[1,3]

[1]National Institute of Polar Research, Research Organization of Information and Systems, 10–3 Midori-cho, Tachikawa, Tokyo 190–8518, Japan, [2]Department of Biological Sciences, Faculty of Science and Engineering, Chuo University, 1-13-27, Kasuga, Bunkyo-ku, Tokyo 112–8551, Japan, [3]Department of Polar Science, School of Multidisciplinary Science, SOKENDAI (The Graduate University for Advanced Studies), 10–3 Midori-cho, Tachikawa, Tokyo 190–8518, Japan, [4]Department of Science and Engineering for Sustainable Innovation, Faculty of Science and Engineering, Soka University, 1–236 Tangi-machi, Hachioji, Tokyo 192–8577, Japan, [5]Nature Research Group, Ehime Prefectural Science Museum, 2133-2 Ojoin Niihama, Ehime 792-0060, Japan, [6]Department of Basic Biology, School of Life Sciences, SOKENDAI (The Graduate University for Advanced Studies), Nishigonaka 38, Myodaiji, Okazaki, Aichi 444–8585, Japan and [7]National Institute for Basic Biology, National Institutes of Natural Sciences, 38 Nishigonaka, Myodaiji, Okazaki, Aichi 444–8585, Japan
**For correspondence. E-mail: kosugi@bio.chuo-u.ac.jp*

Received: 12 March 2018 Returned for revision: 3 May 2018 Editorial decision: 23 June 2018 Accepted: 16 July 2018
Published electronically 23 July 2018

• **Background and Aims** All photosynthetic organisms are faced with photoinhibition, which would lead to death in severe environments. Because light quality and light intensity fluctuate dynamically in natural microenvironments, quantitative and qualitative analysis of photoinhibition is important to clarify how this environmental pressure has impacted ecological behaviour in different organisms.
• **Methods** We evaluated the wavelength dependency of photoinactivation to photosystem II (PSII) of *Prasiola crispa* (green alga), *Umbilicaria decussata* (lichen) and *Ceratodon purpureus* (bryophyte) harvested from East Antarctica. For evaluation, we calculated reaction coefficients, E_{pi}s, of PSII photoinactivation against energy dose using a large spectrograph. Daily fluctuation of the rate coefficient of photoinactivation, k_{pi}, was estimated from E_{pi}s and ambient light spectra measured during the summer season.
• **Key Results** Wavelength dependency of PSII photoinactivation was different for the three species, although they form colonies in close proximity to each other in Antarctica. The lichen exhibited substantial resistance to photoinactivation at all wavelengths, while the bryophyte showed sensitivity only to UV-B light (<325 nm). On the other hand, the green alga, *P. crispa,* showed ten times higher E_{pi} to UV-B light than the bryophyte. It was much more sensitive to UV-A (325–400 nm). The risk of photoinhibition fluctuated considerably throughout the day. On the other hand, E_{pi}s were reduced dramatically for dehydrated compared with hydrated *P. crispa*.
• **Conclusions** The deduced rate coefficients of photoinactivation under ambient sunlight suggested that *P. crispa* needs to pay a greater cost to recover from photodamage than the lichen or the bryophyte in order to keep sufficient photosynthetic activity under the Antarctic habitat. A newly identified drought-induced protection mechanism appears to operate in *P. crispa*, and it plays a critical role in preventing the oxygen-evolving complex from photoinactivation when the repair cycle is inhibited by dehydration.

Key words: Antarctica, drought tolerance, bryophyte, lichens, microclimate, photoinhibition, photosynthesis, photosystem II, *Prasiola*, UV damage.

INTRODUCTION

Light is indispensable to promote photosynthetic reactions. However, all photosynthetic organisms face damage to their electron transport systems due to the formation of excess redox power, resulting in photoinhibition of photosystems and cell death (Aro *et al.*, 1993; Long *et al.*, 1994). Photoinhibition is defined as a decline of photosynthetic activity due to excess light intensity (Kok, 1956). Photoinhibition consists of two physiological phases: deactivation of photosystems mainly due to destruction of the photosystem II (PSII) complex (Aro *et al.*, 1993; Melis, 1999) and recovery of injured photosystems. The recovery phase proceeds simultaneously with the deactivation process, so that photosynthetic activity is maintained as long as the two phases are balanced (Nishiyama *et al.*, 2006; Takahashi and Murata, 2008). However, it is important to analyse the two phases separately, because they are influenced by different environmental factors. In this article, the term 'photoinactivation' is introduced to distinguish it from the traditional term photoinhibition and used to refer to the decline of function of

photosystems by irradiation in the first phase (Oguchi *et al.*, 2009). Also the word 'photodamage' was used for expressing the damage which occurs in photosystems as a consequence of photoinactivation.

Although the processes of photoinactivation have been well studied, these molecular mechanisms have not been fully understood (Aro *et al.*, 1993; Long *et al.*, 1994; Murata *et al.*, 2007; Tyystjärvi *et al.*, 2013). One of the leading hypotheses on the cause of photoinactivation is the disruption of the oxygen-evolving complex (OEC), which consists of an Mn cluster that splits water into molecular oxygen and hydrogen ions (Hakala *et al.*, 2005; Ohnishi *et al.*, 2005). Photoinactivation on the donor side of PSII is primarily induced by short wavelength irradiation, such as ultraviolet (UV) light and blue light (Tyystjärvi *et al.*, 2002; Hakala *et al.*, 2006; Sarvikas *et al.*, 2006). P680 excitation in the PSII complex in which the OEC has been disrupted will induce inactivation of PSII (Ohnishi *et al.*, 2005).

Another mechanism of the photoinactivation process, inactivation of which is initiated on the acceptor side of the PSII reaction centre, has been proposed. This is associated with the photochemical reaction and formation of reactive oxygen species (ROS) such as superoxide anion radical ($\cdot O_2^-$), hydrogen peroxide (H_2O_2), hydroxyl radical (·OH) and singlet oxygen ($^1O_2$). A singlet oxygen is produced by the recombination between $P680^+$ and $pheophytin^-$ (Jones and Kok, 1966; Santabarbara *et al.*, 2001), whereas $\cdot O_2^-$, H_2O_2 and ·OH are produced by transferring electrons from photosystems to oxygen (Asada, 1999; Bondarava *et al.*, 2010; Zulfugarov *et al.*, 2014). The ROS products cause photoinhibition by suppressing protein synthesis in processes of repair from photoinactivation (Nishiyama *et al.*, 2001, 2004; Allakhverdiv and Murata, 2004). Recent studies indicate the ROS induce PSII damage more directly (Hideg *et al*., 2007; Zhang *et al.*, 2011; Zhan *et al.*, 2014; Ding *et al.*, 2016). Photoinactivation in photosystem I (PSI) has also been reported as being induced by an excess electron flow from PSII to PSI, which generates ROS around PSI (Takahashi and Asada, 1988; Jung and Kim, 1990; Terashima *et al.*, 1994; Sonoike *et al.*, 1995; Sonoike, 2011). A slow recovery rate of damaged PSI increases the risk of photoinhibition in PSI, although the possibility of photoinactivation of PSI is much lower than that of PSII under natural conditions (Melis, 1999; Kudoh and Sonoike, 2002; Zhang *et al.*, 2011).

A protein synthesis inhibitor, such as lincomycin or streptomycin, is usually used to analyse net D1 protein degradation by irradiation. In the absence of the inhibitor, this process is obscured by simultaneous synthesis of D1 protein (Xiong and Day, 2001). The amount of D1 protein is decreased exponentially by irradiated light with wavelengths shorter than the blue region, and the damage is expressed as a first-order reaction against integrated irradiation energy with the reaction factor, k_{pi} (Campbell and Tyystjäarvi, 2012). It has been suggested that UV-A (325–400 nm), rather than UV-B radiation (<325 nm) has a stronger effect on degradation of PSII, because total radiation energy in the UV-B region under ambient light is usually much less than that of UV-A at the ground surface (Kondratyev, 1969). The lost activity of PSII caused by UV-B has been estimated to be only 4 % of that caused by UV-A (Hakala-Yatkin and Tyystjärvi, 2011).

Elucidation of the photoinhibition mechanism under normal hydrated conditions of plants or algae has greatly advanced; however, little information on the process of photoinhibition under drought conditions is available. Poikilohydric photosynthetic organisms, such as lichens, bryophytes and aerial algae, can survive under dehydrated conditions for long periods, even if 90 % of the water is lost. Such dehydrated conditions are likely to bring about further risk of photoinhibition to the organisms compared with hydrated conditions. Under such conditions, the life time of photo-oxidized P680 ($P680^+$) would be longer than in a hydrated state due to loss of the electron supply from the OEC, while electrons in the reducing side are evacuated from the PSII complex. This results in the production of a triplet state and then ROS are produced. Because all metabolic activity, including the repair cycle, stops during dehydration, mechanisms that protect against photoinhibition and/or promote rapid metabolic recovery upon rehydration are important for avoiding critical damage.

Drought-tolerant photosynthetic organisms generally have the distinctive characteristic that fluorescence from PSII is specifically quenched on dehydration (Hirai *et al.*, 2004; Heber *et al.*, 2006; Nabe *et al.*, 2007; Kosugi *et al.*, 2009, 2010*a*). The drought-induced non-photochemical quenching (d-NPQ) of PSII is thought to be important for suppressing excitation of the PSII reaction centre, P680. This brings about a low probability of formation of $P680^+$ and the subsequent electron transport. However, there is little information about wavelength dependency of photoinactivation under dehydrated conditions and about the usefulness of the drought tolerance mechanism under natural sunlight. The photoinactivation induced by OEC description on illumination with short wavelength light has rarely been discussed in dehydrated conditions of poikirohydrite phototrophs.

In the continental Antarctic region, photosynthetic organisms are exposed to severely stressful conditions such as low temperatures, strong winds, drought and strong visible (VIS) and UV light in summer. These environmental factors generally accelerate photoinhibition, because the excess reducing power is generated by a limited rate of CO_2 fixation, which slows down or inactivates the repair pathways of photosystems (Powles, 1984; Murata *et al.*, 2007). In addition, photosynthetically active periods during the Antarctic summer are rather short so that the organisms in those areas are not at an advantage in terms of energy balance. It is highly plausible that lichens, bryophytes and algae in Antarctica possess high potential to avoid photoinhibition under severe environments. However, th physiological and ecophysiological mechanisms of this adaptive strategy to avoid photoinhibition remain unclear.

In this study, we determined the reaction coefficients (E_{pi}s) of photoinactivation and compared the wavelength dependency among a green alga [*Prasiola crispa* (Lightfoot) Kützing], a lichen [*Umbilicaria decussata* (VILL.) ZAHLBR.] and a bryophyte [*Ceratodon purpureus* (Hedw.) Brid.)] that were collected at Langhovde on the Sôya Coast in East Antarctica. All the species are drought tolerant and can construct large colonies in Antarctic terrestrial habitats (Longton, 1988; Kanda and Inoue, 1994; Kosugi *et al.*, 2010*a*). From measurements of fluorescence yield, it was possible to determine the reaction coefficients of PSII photoinactivation and to estimate the costs needed for the recovery from photodamage occurring under natural conditions. The cost for maintaining photosynthetic activity can be

defined as an environmental pressure, and estimation of the pressure is important for revealing their adaptation strategies in severe environments.

MATERIALS AND METHODS

Collection of samples and measurements of the light environment

Photosynthetic organisms for laboratory experiments were collected at Yukidori Zawa and Yotsuike Dani in Langhovde on the Sôya Coast, East Antarctica, in January 2013 (Fig. 1). Yukidori Zawa is designated as an Antarctic Specially Protected Area (ASPA No. 141) because of its lush vegetation. We selected an observation and sampling site in Yukidori Zawa (69°14′24.90″S, 39°44′20.16″E) at 88 m asl (Kosugi *et al.*, 2015). This site is located on the northern slope of the valley, and an automatic weather station (69°14′28″S, 39°44′21″E) had previously been set up near the site (Kudoh *et al.*, 2015*a*, *b*). Several lichens and large moss colonies spread in a wide range around the rock, and macrophytic soil algae were found near the rock. We selected a lichen (*Umbilicaria decussata*), a moss (*Ceratodon purpureus*) and a green alga (*Prasiola crispa*) as our research materials. These three species were the most dominant of the lichens, mosses and

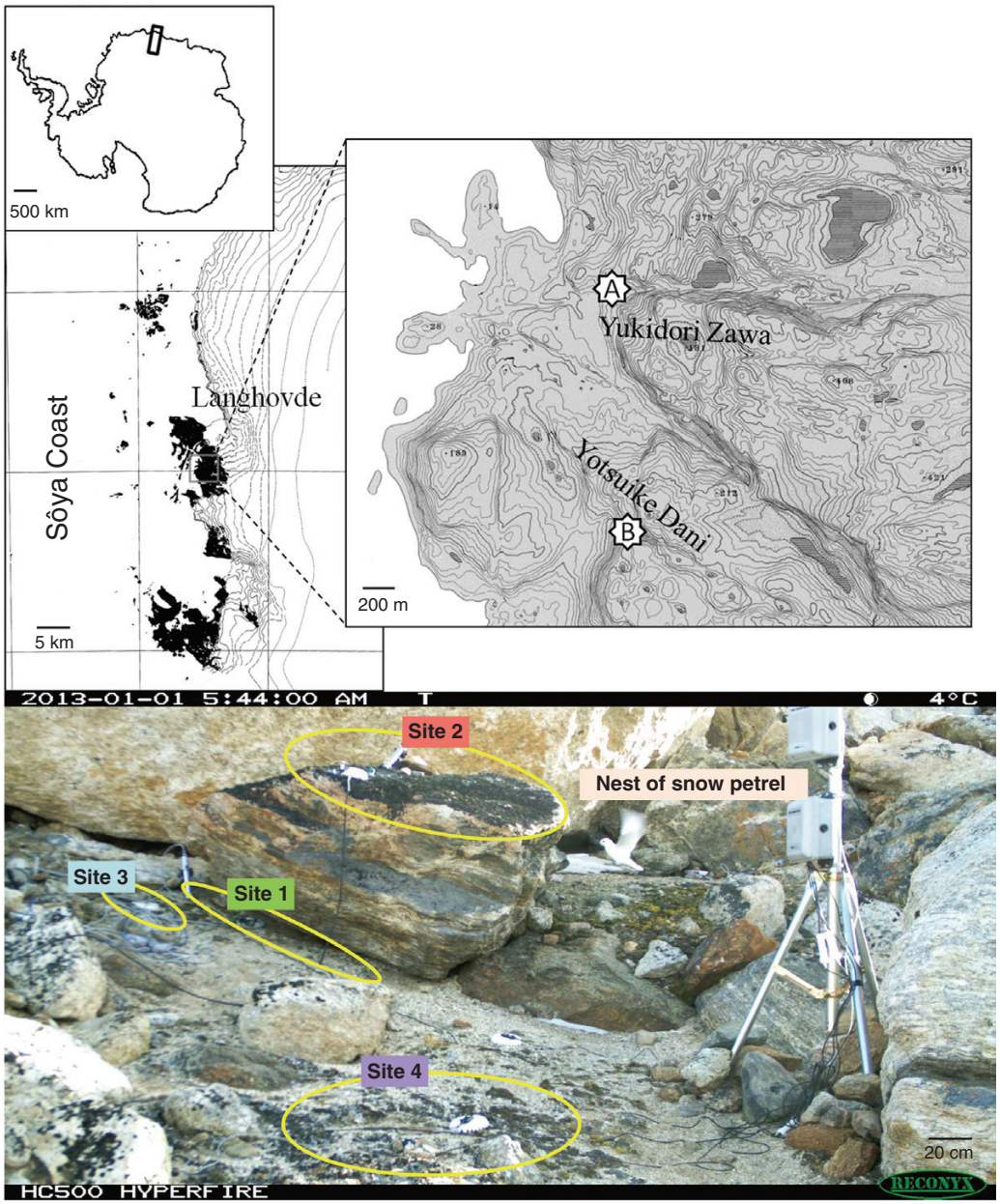

FIG. 1. Maps of the study site. The study site was located in Langhovde on the Sôya Coast, East Antarctica. Point A at Yukidori Zawa shows the observation and sampling point. Point B at Yotsuike Dani shows another sampling point. The original base map was published by the Geospatial Information Authority of Japan in 1968 and 1978. The photograph was taken by a stationary camera set up at point A. It shows observation sites: Site 1, a habitat of *P. crispa*; Site 2, a habitat of *U. decussata*; Site 3, a habitat of *C. purpureus*; and Site 4, a habitat of *C. purpureuse* and lichens.

aerial algae found at the site. Additional samples of *P. crispa* were collected at Yotsuike Dani (69°15′25″S, 39°44′40″E) at approx. 120 m asl. All samples were dehydrated in the shade and stored at −20 °C while being transported to the laboratory.

Sunlight spectra were measured spectrophotometrically on 2 January 2013 near the *P. crispa* habitat and in an open site close to its habitat, where *U. decussata* and *C. purpureus* were found in both sites. We used a spectrophotometer (Ramses-ACC-VIS; TriOS Mess- und Datentechnik GmbH, Rastede, Germany) that covered the wavelength range of 280–720 nm, with a spectral accuracy of 0.3 nm. Integration time was 8 s.

Experimental irradiation analysis by a large spectrograph

Samples were rehydrated and washed with Milli-Q water at 4 °C to remove sand from the thalli. They were then dehydrated again at 4 °C in the dark for about 1 week and subsequently stored at −20 °C until required for experiments.

Umbilicaria decussata thalli were cut into small pieces of approx. 25 mm^2 and attached to black paper with double-sided tape. *Ceratodon purpureus* shoots were tied into ten-shoot bundles with string and stood upright to mimic natural conditions. Sheet-like colonies of dehydrated *P. crispa* were homogenized in a blender (to pieces of approx. 2 mm in diameter) and divided into 50 mg samples. Preliminary experiments indicated that there was little difference between the ground and non-ground samples in terms of photochemical signals. Chlorophyll extraction was performed using 100 % methanol after grinding hydrated samples using a mortar and pestle. For determination of the average chlorophyll content, we used 15 pieces of about 0.7 cm^2 (five pieces were cut from one thallus) for *U. decussata*, ten pieces of about 0.5 cm^2 for *C. purpureus* and three samples of about 0.7 cm^2 homogenized in a blender for *P. crispa.* Area calculations were performed by means of Image J (NIH, MD, USA). Chlorophyll content per unit area was calculated according to Porra *et al.* (1989) as 14.18 ± 6.89 (± s.d.), 22.81 ± 3.77 and 15.57 ± 1.29 μg Chl cm^{-2} in *U. decussate*, *C. purpureus* and *P. crispa*, respectively.

The samples were exposed to monochromatic light using the Okazaki large spectrograph at the National Institute for Basic Biology (Watanabe *et al.*, 1982; Watanabe, 1995). The spectrum of light dispersed by the diffraction grating had a bandwidth of about 10 mm per 1 nm at the irradiation stage. The light of ±4.5 nm at a given target wavelength was reflected by a mirror, collected by a 90 mm lens and exposed to the samples vertically. The energy flux density was controlled by neutral density filters. Twelve wavelengths were selected between 320 and 750 nm. Among them, 435, 470 and 660 nm were selected as the chlorophyll *a* and *b* absorption bands. Light intensity was regulated by a monochromatic quantum sensor, QTM-101 (Monotech Inc., Saitama, Japan). For the hydrated samples, we used 35–100 and 75–200 μmol photons m^{-2} s^{-1} for UV and VIS radiation, respectively. For the dehydrated samples, we used 35–1000 and 200–2000 μmol photons m^{-2} s^{-1} for UV and VIS radiation, respectively. Because the dehydrated samples showed much higher resistance relative to that of the hydrated samples, a stronger light intensity was necessary to obtain a significant photoinhibition for calculating reaction parameters. We used several light intensities that were converted to energy dose, kJ m^{-2}, to calculate reliable reaction coefficients, E_{pi}s.

For exposure of monochromatic light using wet samples, each sample was dipped in 50 mM MES buffer (pH 5.5) containing 1.0 mg mL^{-1} streptomycin at 10 °C in the dark for 2 h to inhibit the PSII repair cycle (Schnettger *et al.*, 1994; Xiong, 2001; Xiong and Day, 2001). The samples were then set on a sample stand that was equipped with a cooling block kept at 10 °C. Room temperature was set at 17 °C. Because cool treatment sometimes induces dew formation during incubation, exposure of the dehydrated samples to monochromatic light was performed at room temperature (17 °C) without a cooling block. We confirmed that treatment at 17 °C under dehydrated conditions had no effect on photosynthetic activity after rehydration.

Chlorophyll fluorescence measurement and photodamage evaluation

Maximum PSII quantum yield, expressed as a fluorescence parameter, F_v/F_m, was measured by a pulse amplitude modulation chlorophyll fluorometer, PAM-2100 (Heinz Walz GmbH, Effeltrich, Germany). The intensity of the measuring light and the saturation pulse were 0.17 and 5000 μmol photons m^{-2} s^{-1}, respectively. The duration of the saturation pulse was set to 0.8 s. The three samples show their maximum fluorescence value by this saturation pulse. Samples were dark adapted for 30 min after irradiation treatment of the hydrated samples. This dark adaptation period allows full relaxation of photoinduced reactions including state transition. In the case of the dehydrated samples, rehydration treatment with streptomycin-containing buffer was performed for 2 h under dark/cool conditions (10 °C) before measurement. Measurements were performed under weak green light to avoid the activation of photosynthesis. All samples were kept at 10 °C during the fluorescence measurements.

Damage to PSII is expressed as the magnitude of photoinactivation, and the degree of damage is indicated by the parameter of maximum PSII fluorescence yield, F_v/F_m. The F_v/F_m value reflects the electron transport capacity of PSII, and its decline following exposure to monochromatic light indicates a decline of PSII activity (Krause and Weis, 1991). A decline in F_v/F_m by photoinactivation is a first-order reaction against exposure time in the presence of a protein synthesis inhibitor, and it can be expressed by the following equation, with k_{pi} as the rate constant of the reaction (Wünschmann and Brand, 1992; Tyystjärvi *et al.*, 1994; Tyystjärvi and Aro, 1996):

$$y = a \times e^{-k_{pi} \times t} \quad (1)$$

where a is the constant (= 1, for the present experimental setting) determined by the ratio of a non-damaged sample of zero dose as $(F_v/F_m)_{non\text{-}exposed}/(F_v/F_m)_{non\text{-}exposed} = 1$, and y is the fraction of active PSII determined by $(F_v/F_m)_{exposed}/(F_v/F_m)_{non\text{-}exposed}$ at time t. Here, it was known that k_{pi} is dependent on both wavelength of a photon and the number of photons. It means that k_{pi} can be replaced as a reaction coefficient against photon flux density (n) or against energy flux density (I; with units of W m^{-2}) when monochromatic light is used for irradiation treatment.

$$y = a \times e^{-N_{pi} \times n \times t}$$

or

$$y = a \times e^{-E_{pi} \times I \times t} \quad (2)$$

Thus, the value '$E_{pi} \times I$' is defined as a rate coefficient of photoinactivation.

$$E_{pi} \times I = k_{pi} \quad (3)$$

The $n \times t$ and the $I \times t$ can be converted to a total number of photons (N) and a total energy dose (x; with units of J m^{-2}), respectively.

$$y = a \times e^{-N_{pi} \times N}$$

$$y = a \times e^{-E_{pi} \times x} \quad (4)$$

N_{pi} and E_{pi} are defined as reaction coefficients of photoinactivation in PSII against the total numbers of photons and total energy dose, respectively. These reaction coefficients depend on the wavelength of light.

The PSII photoinactivation ratio is defined as $[1-(F_v/F_m)_{exposed}/(F_v/F_m)_{non\text{-}exposed}]$:

$$\begin{aligned}\left(\text{fraction of photoinactivation}\right) &= 1 - a \times e^{-E_{pi} \times I \times t} \\ &= 1 - a \times e^{-k_{pi} \times t}\end{aligned} \quad (5)$$

A rate constant of photoinactivation under an ambient light source was calculated as the summation of k_{pi} for each wavelengths, $\sum_{320nm}^{660nm} \left\{\left(E_{pi}\right)_\lambda \times I_\lambda\right\}$. For estimation of rate constants of photoinactivation under ambient light, k_{pi}s were determined at the selected wavelengths: λ = 320, 340, 360, 380, 435, 470, 500, 550, 600 and 660 nm. After determination of $\left(E_{pi}\right)_\lambda$ at the respective wavelengths, the light intensities of ambient light at specific wavelengths were multiplied $E_{pi(\lambda\,=\,320)} \times \Delta I_{300\text{–}330}$, $E_{pi(\lambda\,=\,340)} \times \Delta I_{330\text{–}350}$, $E_{pi(\lambda\,=\,360)} \times \Delta I_{350\text{–}370}$, $E_{pi(\lambda\,=\,380)} \times \Delta I_{370\text{–}400}$, $E_{pi(\lambda\,=\,435)} \times \Delta I_{400\text{–}460}$, $E_{pi(\lambda\,=\,470)} \times \Delta I_{460\text{–}480}$, $E_{pi(\lambda\,=\,500)} \times \Delta I_{480\text{–}520}$, $E_{pi(\lambda\,=\,550)} \times \Delta I_{520\text{–}570}$, $E_{pi(\lambda\,=\,600)} \times \Delta I_{570\text{–}640}$ and $E_{pi(\lambda\,=\,660)} \times \Delta I_{640\text{–}680}$. Finally the rate constant under ambient light $\sum_{320nm}^{660nm} \left\{\left(E_{pi}\right)_\lambda \times I_\lambda\right\}$ was calculated.

Statistics

We calculated the standard errors of E_{pi}, and statistical tests were done by evaluating t-values and P-values as below. The parameter E_{pi} is defined as a regression coefficient (b) in eqn (6) derived from eqn (4).

$$\therefore \ln y = y' = \ln a - b \times x \,(b = E_{pi}) \quad (6)$$

The regression coefficient (b) and the regression constant (a) are calculated as eqns (7) and (8)

$$b = \frac{s_{xy'}^2}{s_x^2}\left(s_{xy}^2, \text{unbiased covariance}; s_x^2 : \text{unbiased variance}\right) \quad (7)$$

$$a = \bar{y}' - b\bar{x}.\,(\bar{y}' \text{and } \bar{x}, \text{sample means})$$

The s.e. (s_b) of the regression coefficient is calculated as in eqn (9). The regression coefficient (b) was evaluated in a test of statistical significance against a null hypothesis H_0:b = 0 by using the t-value (t_b), eqn (10)

$$s_b = \sqrt{\frac{\sum_{i=1}^{n} \frac{d_{xy'}^2}{\{(n-1)(n-2)\}}}{s_x^2}}. \quad (9)$$

($d_{xy'}^2$, total sum of squares)

$$t_b = \frac{b}{s_b} \quad (10)$$

Coefficients of determination (r^2) were calculated from r-values between y' and x in eqn (6) as Pearson's correlation coefficient, eqn (11).

$$r = \frac{\frac{\left\{\sum_{i=1}^{n}\left(X_i - \bar{X}\right)(Y'_i - \bar{Y}')\right\}}{(n-1)}}{S_x S_{y'}}. \quad (11)$$

(s_x and $s_{y'}$: standard deviations)

P-values of b (E_{pi}s) were evaluated from t-values. E_{pi}s, s.e., P-values and r^2-values are shown in Table 1, and s.e. vlues of E_{pi}s are shown as error bars in Fig. 4.

Evaluations of k_{pi} *and* k_{rec} *under sunlight conditions*

We used a solar simulator HAL-C100 (Asahi Spectra, Tokyo, Japan) with a quartz light guide (φ5 × 1000 mm) and a rod lens, RLQ80-05 (Asahi Spectra), for comparing k_{pi} and k_{rec} under sunlight conditions with those estimated under the spectrum exposure experiments explained in the previous sections. Dehydrated thalli of *P. crispa* which were ground into small pieces in advance were hydrated with 50 mM MES buffer (pH 5.5) ± 1.0 mg mL^{-1} streptomycin for 2 h under dark conditions and spread evenly in the bottom of a small aluminium dish (2 × 1 cm × H 1 cm). The dish was put on an aluminium block of a cooling dry bath incubator, MC-0203 (Major Science, CA, USA), and was irradiated with artificial sunlight for the given times. The incubation temperature was set to 15 °C. The light intensity was modulated by changing the distance between the rod and the sample or changing the built-in ND filters. The exact exposure intensities were checked by a light meter, LI-250A, and a photochemically active radiation (PAR) sensor, LI-190R (LI-COR, Lincoln, NE, USA). The spectral intensity of each wavelength was calculated using the relative energy spectrum intensity of the artificial light source which was specified by the manufacturer, and the PAR exposures are listed in Table 2.

Measurement of algal absorption spectra

The absorptance spectrum of *P. crispa* thalli was calculated as

$$\text{Absorptance} = 1 - \left(\text{Reflectance} + \text{Transmittance}\right)$$

TABLE 1. *Reaction factors of PSII damage,* E_{pi}*s, and statistical factors*

WL (nm)	Reaction factors		Coefficient of determination	WL (nm)	Reaction factors		Coefficient of determination
	E_{pi} (×10^{-4}) ± s.e.	*P*	r^2		E_{pi} (×10^{-4}) ± s.e.	*P*	r^2
Prasiola crispa (hydrated)*				*P. crispa* (dehydrated)†			
320	38.68 ± 3.12	<0.001	0.88	320	2.36 ± 0.21	<0.001	0.85
340	27.26 ± 2.01	<0.001	0.90	340	1.95 ± 0.11	<0.001	0.94
360	31.97 ± 3.97	<0.001	0.77	360	1.49 ± 0.09	<0.001	0.9
380	15.57 ± 2.59	<0.001	0.66	380	1.30 ± 0.13	<0.001	0.81
435	3.71 ± 0.85	<0.001	0.34	435	0.60 ± 0.07	<0.001	0.78
470	2.60 ± 0.59	<0.001	0.35	470	0.50 ± 0.05	<0.001	0.83
500	1.71 ± 0.71	<0.05	0.14	500	0.68 ± 0.05	<0.001	0.90
550	0.18 ± 0.56	>0.1	0.00	550	0.49 ± 0.09	<0.01	0.58
600	1.51 ± 0.67	<0.05	0.12	600	0.50 ± 0.09	<0.01	0.59
660	3.65 ± 0.94	<0.001	0.18	660	0.20 ± 0.08	<0.1	0.21
750	–3.35 ± 0.93	>0.1	0.26	750	0.01 ± 0.06	>0.1	0.00
Ceratodon purpureus‡				*Umbilicaria decussata*‡			
320	5.66 ± 1.03	<0.01	0.88	320	–0.32 ± 0.37	>0.1	0.16
340	1.40 ± 0.83	>0.1	0.51	340	1.38 ± 0.87	>0.1	0.46
360	0.54 ± 0.32	>0.1	0.41	360	0.37 ± 0.98	>0.1	0.18
380	0.44 ± 0.43	>0.1	0.16	380	–0.95 ± 1.23	>0.1	0.13
435	0.08 ± 0.24	>0.1	0.13	435	–0.26 ± 0.35	>0.1	0.12
470	–0.20 ± 0.23	>0.1	0.15	470	–0.66 ± 0.21	<0.05	0.72
500	–0.12 ± 0.24	>0.1	0.06	500	–0.83 ± 0.43	>0.1	0.48
550	–0.36 ± 0.2	>0.1	0.44	550	–0.48 ± 0.41	>0.1	0.26
600	–0.08 ± 0.23	>0.1	0.03	600	–0.03 ± 0.84	>0.1	0.00
660	0.81 ± 0.33	>0.1	0.61	660	0.08 ± 0.26	>0.1	0.02
750	–1.30 ± 0.28	<0.01	0.84	750	–2.19 ± 0.32	<0.001	0.92

Reaction factors of PSII damage, E_{pi}s, were obtained from least squares regression of the PSII recovery rate in a first-order reaction against the irradiation energy dose.

Standard errors, *P*-values in statistical hypothesis testing and coefficients of determination (r^2) for each wavelength (WL) were calculated as described in the Materials and Methods.

*320–380 nm, n = 21; 435–750 nm, n = 39.

†320–750 nm, n = 24.

‡320–750 nm, n = 6,

TABLE 2. *Irradiation doses in each wavelength range of the artificial light source at three different PAR exposure conditions for 10, 20 and 30 min*

Wavelength (nm)		260 μmol photons m^{-2} s^{-1}			580 μmol photons m^{-2} s^{-1}			1750 μmol photons m^{-2} s^{-1}		
		10 min	20 min	30 min	10 min	20 min	30 min	10 min	20 min	30 min
	(integrated area)	kJ			kJ			kJ		
320	300–330	1.27	2.54	3.82	2.56	5.12	7.68	7.79	15.57	23.36
340	330–350	1.04	2.08	3.12	2.09	4.19	6.28	6.37	12.74	19.11
360	350–370	1.42	2.84	4.26	2.86	5.72	8.57	8.70	17.40	26.09
380	370–400	3.94	7.88	11.81	7.92	15.83	23.75	24.09	48.19	72.28
435	400–460	4.81	9.62	14.44	9.67	19.35	29.02	29.44	58.88	88.33
470	460–480	4.72	9.44	14.15	9.49	18.97	28.46	28.87	57.74	86.61
500	480–520	6.82	13.64	20.46	13.71	27.42	41.13	41.72	83.45	125.17
550	520–570	6.48	12.96	19.44	13.03	26.06	39.10	39.66	79.32	118.98
600	570–640	7.20	14.40	21.60	14.47	28.95	43.42	44.05	88.10	132.14
660	640–680	4.42	8.84	13.26	8.88	17.77	26.65	27.04	54.08	81.12

Irradiation doses in each wavelength range of a solar simulator HAL-C100 were calculated using the relative energy spectrum intensity of the artificial light source and the PAR of exposure.

The light intensity was modulated by changing the distance between the rod and the sample or changing the built-in ND filters.

The transmittance was measured with a spectrophotometer, MPS-2000 (Shimadzu, Kyoto, Japan). A piece of the sheet-like *P. crispa* algal colony was placed on the outside of a quartz cell as follows: the algal body was fixed by two pieces of cellophane tape to set the sample in the light path. The quartz cell with the sample was set in front of the photomultiplier, to minimize the scattering of the measuring beam by the algal cells. Reflectance was measured by UV-2600 (Shimadzu) with an integrating sphere, ISR-2600 Plus (Shimadzu). The sheet-like thalli were held between two quartz grass filters (50 × 50 × 1 mm) and set

in the spectrometer. The blank value was measured with water held between two quartz glass sheets.

RESULTS

Wavelength dependency of photoinhibition

We exposed samples to two different energy flux densities, using 100 and 200 µmol photons m^{-2} s^{-1} for the UV (320–380 nm) and VIS (435–750 nm) spectral regions. The exposure time necessary to induce a significant photoinactivation was then determined; it was 1 h for *P. crispa* and 5 h for both *U. decussata* and *C. purpureus*. Figure 2 shows the wavelength dependency of the maximum quantum yield of PSII for the three photosynthetic organisms on the exposure treatments. Damage was detected and enhanced when the hydrated samples from all three species were exposed to 100 µmol photons m^{-2} s^{-1} of UV radiation for 1–5 h. Notably, >40 % of the fluorescence yield was lost in *P. crispa* after 1 h of exposure to UV radiation. This result indicates that *P. crispa* is highly sensitive to UV exposure. However, *U. decussata* and *C. purpureus* retained >80 % of the fluorescence yield at all wavelengths, except for the 320 nm exposure in *C. purpureus*. Exposure to VIS at 200 µmol photons m^{-2} s^{-1} for 5 h did not induce significant photoinactivation for hydrated *U. decussata* and *C. purpureus*, but 10–20 % damage was detected in *P. crispa* that were exposed to blue light at 435 and 470 nm for 1 h (Fig. 2). The F_v/F_m ratios were higher after irradiation with light at 750 nm for all samples. This is presumably due to oxidation of the plastoquinone pool by far-red irradiation, which selectively excites PSI (Asada *et al.*, 1992, 1993). This would bring about an apparently higher quantum yield of PSII (Kurreck *et al.*, 2000).

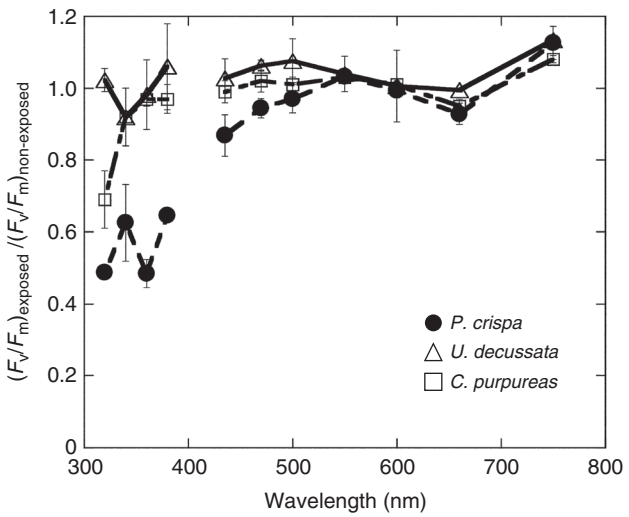

FIG. 2. Wavelength dependency of photoinactivation in the three test organisms. PSII photoinactivation by different bands of the light spectrum of the samples in the hydrated state. Samples were illuminated at 100 and 200 µmol photons m^{-2} s^{-1} for UV bands (320–380 nm) and visible light bands (435–750 nm). Illumination times were set to 1–5 h for *P. crispa* and the the other two organisms. Each point shows the average value of three samples, and error bars indicate the s.d. (n = 3).

Mathematical expression of photoinactivation of the Prasiola crispa *PSII*

Wavelength-dependent photoinactivation in response to different energy doses was analysed in more detail for *P. crispa* to evaluate the relationship under hydrated and dehydrated conditions. The hydrated samples were exposed to two energy flux densities of 35 and 75 µmol photons m^{-2} s^{-1} for the UV spectral region and three energy flux densities of 75, 100 and 200 µmol photons m^{-2} s^{-1} for the VIS spectral region, respectively. The dehydrated samples were exposed to two energy flux densities for the UV spectral region (100 and 1000 µmol photons m^{-2} s^{-1}) and two energy flux densities for the VIS spectral region (100 and 2000 µmol photons m^{-2} s^{-1}). Irradiation time was set to 30–120 and 30–180 min for hydrated and dehydrated samples, respectively. We calculated the integrated energy dose (kJ m^{-2}) from the photon flux density and irradiation time. Figure 3 shows the relationship between PSII damage and radiation energy dose for different wavelengths. Figure 3A and C shows the results of UV light exposure for hydrated and dehydrated samples, respectively, and Fig. 3B and D shows those of VIS exposure for hydrated and dehydrated samples, respectively. Photoinactivation was induced along with increased energy dose in all monochromatic light, but steep declines with energy dose were evident for UV exposures in the hydrated samples (Fig. 3A). Fluorescence yield decreased in the dehydrated samples when exposed to UV light (Fig. 3C), while it decreased more steeply in the hydrated samples (Fig. 3A). Although the fluorescence yield decreased in the dehydrated sample, the energy dose necessary to induce similar photoinactivation was close to ten times higher (Fig. 3C). These results indicate that dehydrated samples have higher resistance against both UV and VIS irradiation. VIS exposure had little effect on the quantum yield of PSII in both the hydrated and dehydrated samples.

We could calculate the reaction coefficient E_{pi} from data in Fig. 3. The PSII photoinactivation reaction coefficients, E_{pi}s, at each wavelengths, as calculated by eqn (4), are summarized in Table 1. The s.e. of E_{pi}, the P-value and the coefficient of determination (r^2) were calculated statistically as is described in the Materials and Methods. The P-values show the probability that the null hypothesis, H_0: E_{pi} = 0, is true. The coefficient of determination shows a goodness of fit to the regression equation. Notably, the E_{pi} at 320 nm (E_{pi} = 38.7 × 10^{-4} kJ^{-1} m^2) was 2.5 times higher than that at 380 nm (E_{pi} = 15.6 × 10^{-4} kJ^{-1} m^2) in the hydrated samples. The coefficients at the boundary between the UV and VIS spectral regions (i.e. between 380 and 435 nm) were quite different, with the ratios being >4 (Table 1). However, dehydrated *P. crispa* exhibited high UV and VIS radiation tolerance; the E_{pi} at 320 nm (E_{pi} = 2.4 × 10^{-4} kJ^{-1} m^2) was 16 times smaller than that of the hydrated samples. In order to compare reaction coefficients, the E_{pi}s at each wavelength were calculated for dehydrated *P. crispa* based on the data in Table 1 and for hydrated *U. decussata* and *C. purpureus* using the data in Fig. 2. The E_{pi}s are depicted in Fig. 4 as a function of wavelength. At wavelengths longer than 435 nm, the hydrated *P. crispa* reaction coefficients did not differ compared with either of the other species or conditions. However, it increased sharply at wavelengths shorter than 380 nm. On the other hand, E_{pi}s of dehydrated *P. crispa* and hydrated *U. decussata* and *C. purpureus* were small at all wavelengths. This result

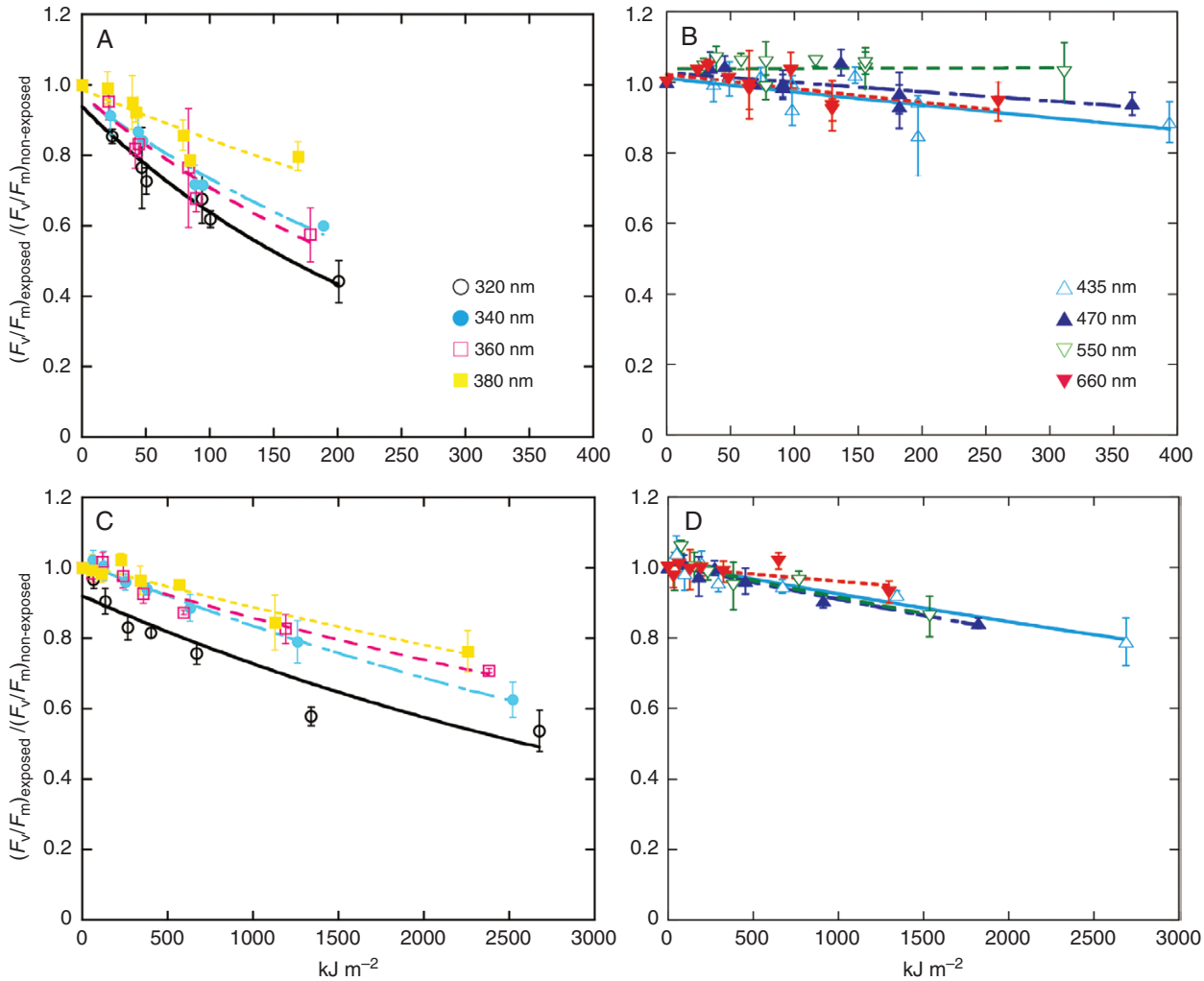

FIG. 3. Relationship between photoinactivation (decrease in PSII quantum yield) and energy dose at each wavelength. PSII photoinactivation in *P. crispa* was measured against the dose of irradiation in UV regions (A and C) (at 320, 340, 360 and 380 nm) and VIS regions (B and D) (435, 470, 500 and 660 nm). Hydrated and dehydrated conditions are shown in (A), (B) and (C), (D), respectively. Measuring points of each wavelengths were fitted to a first-order reaction equation. Each point shows the average value of three samples, and error bars indicate the s.d. ($n = 3$).

suggests that hydrated *P. crispa* is rather sensitive to photoinactivation by UV irradiation. A small peak of E_{pi} is found at around 360 nm (Fig. 4). The wavelength dependency of photoinactivation is affected by the absorption spectra of thalli. When the irradiated light is absorbed by pigments such as chlorophylls or carotenoids, photons do not reach the OEC and it will avoid destruction. Chlorophylls have absorption bands in the blue and red light regions, and carotenoids have absorption maxima at approx. 400–550 nm. Absorption by UV-shielding substances, such as mycosporine-like amino acids (MAAs), peaks at approx. 320 nm (Hoyer *et al.*, 2001; Rozema *et al.*, 2002). The absorptance spectrum of *P. crispa* (Fig. 4) shows a valley at 360 nm as a result of the sum of these pigments. This window will additively increase the radiation dose to the OEC in this wavelength range and could induce the small peak. In fact, the E_{pi} has a distinct peak at this wavelength. The E_{pi} estimated in this study was significantly higher in the UV region for hydrated *P. crispa* ($P < 0.001$), but it became lower in the VIS region, and was low to zero at 550 nm. Although a numerical value was obtained, it was practically zero since the *P*-value was >0.1. Other values were significantly higher than zero (<0.5) except at 750 nm where it was negative. A possible reason for the increase in F_v/F_m at 750 nm was mentioned earlier. It should be kept in mind that the coefficients of determinations are low at wavelengths longer than 500 nm. The low values of both coefficients of determination (<0.5) and E_{pi} (<2.0×10^{-4}) were distinguished at 500, 550 and 600 nm in Table 1, and indicated that the variations of values were caused by individual differences rather than the effect of irradiation. On the other hand, at 660 nm, the low values of coefficients of determination and high values of the E_{pi} and its *P*-value indicated that a decrease in yield of PSII by irradiation could be caused by an effect other than photoinactivation derived from disruption of the OEC.

In dehydrated *P. crispa*, strong correlation of E_{pi} with eqn (4) was obtained in the VIS light region, except at 750 nm. Although E_{pi} values were small, *P*-values were all ≤0.1, except at 750 nm. *Ceratodon purpureus* showed a relatively high correlation at 320 nm and the E_{pi} value was also significantly higher. However, the values at other wavelengths were so small that they were practically zero (>0.1). This indicates

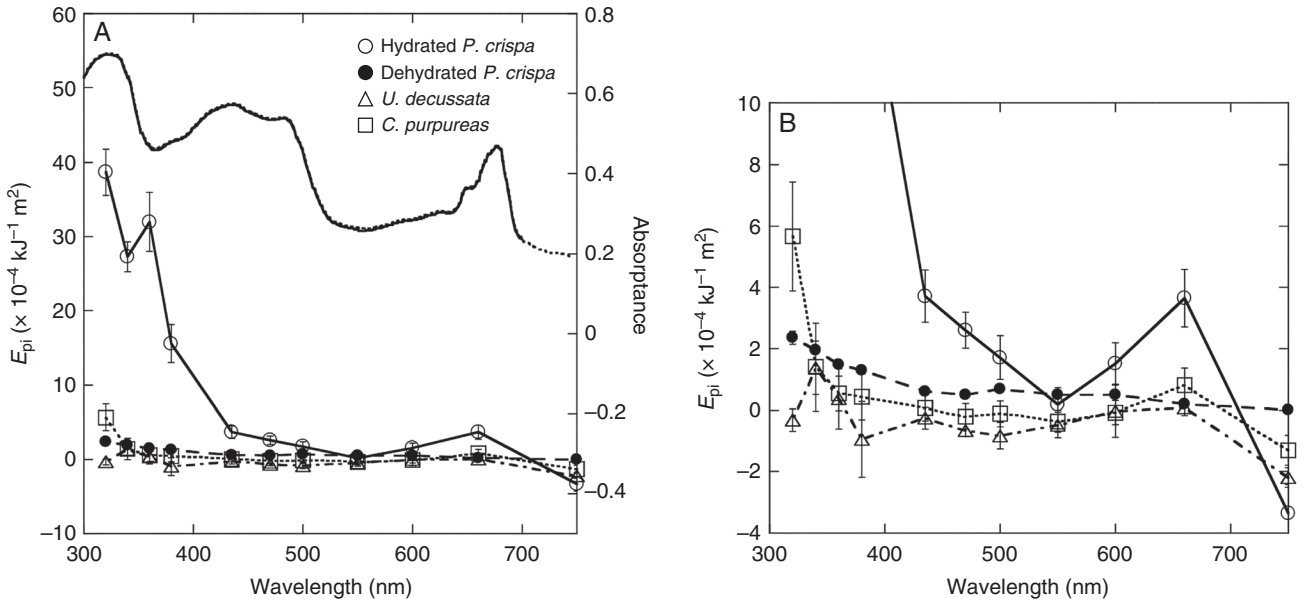

FIG. 4. Wavelength dependency of reaction factors, E_{pi}s, and an absorptance spectrum of hydrated *P. crispa*. Reaction coefficients of PSII inactivation against irradiation dose in hydrated *P. crispa*, dehydrated *P. crispa*, *U. decussata* and *C. purpureus* were plotted against wavelength. An absorptance spectrum of hydrated *P. crispa* is shown as a solid line. The dotted line shows a spectrum of absorptance. (B) Expansion of the ranges <1.0 × 10^{-3} of E_{pi}. The error bars indicate the s.e. as shown in Table 1.

that *C. purpureus* is almost resistant to UV-A or visible light illumination. This was the same in *U. decssata*; moreover, this lichen also showed high resistance to UV-B (320 nm).

Estimation of photoinactivation under natural conditions

Using the E_{pi} at each wavelength (see Table 1) and the spectral energy flux density data, we estimated the degree of photoinactivation in the hydrated or dehydrated state under the ambient Antarctic sunlight of midsummer. Sunlight spectra were measured at the open site, which was exposed to direct sunlight during the day (Fig. 5A), and near Site 1 where *P. crispa* was growing (Fig. 5B). Measurements were performed on 2 January, when the weather was fine and the sky was clear all day. Similar spectra and intensities were observed between 08.00 and 18.00 h at the open site (Fig. 5A). However, the spectral properties differed considerably at the *P. crispa* habitat, because it was shaded from direct sunlight by a rock in the morning. Site 1 was blocked from direct sunlight (Fig. 5B, 8.00 and 12.00 h), but the site was exposed after 14.00 h. The energy distribution spectrum exhibited a similar pattern to that observed at the open site in the afternoon.

We calculated the rate constant of photoinactivation against the exposure time, $k_{pi} = \{E_{pi} \times I\}$, which is defined as the effective photoinactivation dose under ambient light spectra, where I is the energy flux density. Figure 6 shows the wavelength dependency of k_{pi} against the sunlight spectra at noon (12.00 h) for the hydrated *P. crispa*, *U. decussata* and *C. purpureus*, and dehydrated *P. crispa* in the open site (Fig. 6A) and the *P. crispa* habitat (Fig. 6B). Diurnal variation of the rate constant (k_{pi}) at each wavelength for all samples is shown in Fig. 7. At the open site, maximum photoinactivation was calculated to be induced at around 360 nm of light at noon for hydrated *P. crispa*, while it was greatly suppressed for hydrated *U. decussata* and *C. purpureus* between 320 and 660 nm (Figs 6A and 7A, E, G). For hydrated *P. crispa* in its natural habitat, the degree of photoinactivation was quite low during the sun-shaded period (08.00–12.00 h, see Fig. 7B); maximal photoinactivation was estimated to be induced at 360 nm light. The k_{pi} values were also greatly suppressed at 320 nm (Figs 6B and 7B). After 12.00 h, direct sunlight reached the habitat of *P. crispa*, and the k_{pi} values increased to levels similar to those at the open site (Fig. 7A, B).

The integrated values of k_{pi} from 320 to 660 nm can be calculated as the area of the spectrum of wavelength dependency of k_{pi} shown in Fig. 6. This will indicate the rate constant of each specimen under ambient light of Antarctica. Diurnal changes in the total effective photoinactivation dose of each sample are depicted in Fig. 8. This parameter was seven times larger for hydrated *P. crispa* (Fig. 8, open circles with solid line) than those of *U. decussata* and *C. purpureus* at the open site. However, the parameters for *P. crispa* at the habitat were suppressed to one-eighth of those of the open site between 08.00 and 12.00 h (Fig. 8, open circles with dashed line). The total effective photoinactivation doses for *U. decussata* and *C. purpureus* were close to zero at the habitat in the morning. The rate constant increased in the afternoon as for *P. crispa*, but the magnitude of change was much smaller.

Hydrated *P. crispa* is sensitive to irradiation compared with dehydrated *P. crispa* and the other two species, so it faces a high risk of damage by photoinhibition in the daytime in summer. Taking into account the fact that *P. crispa* propagates and develops colonies at the habitat under irradiated conditions, the repair system seems to be working well since the thalli or colony are maintained at the habitat; otherwise the colony would diminish and finally disappear. Evaluation of the rate

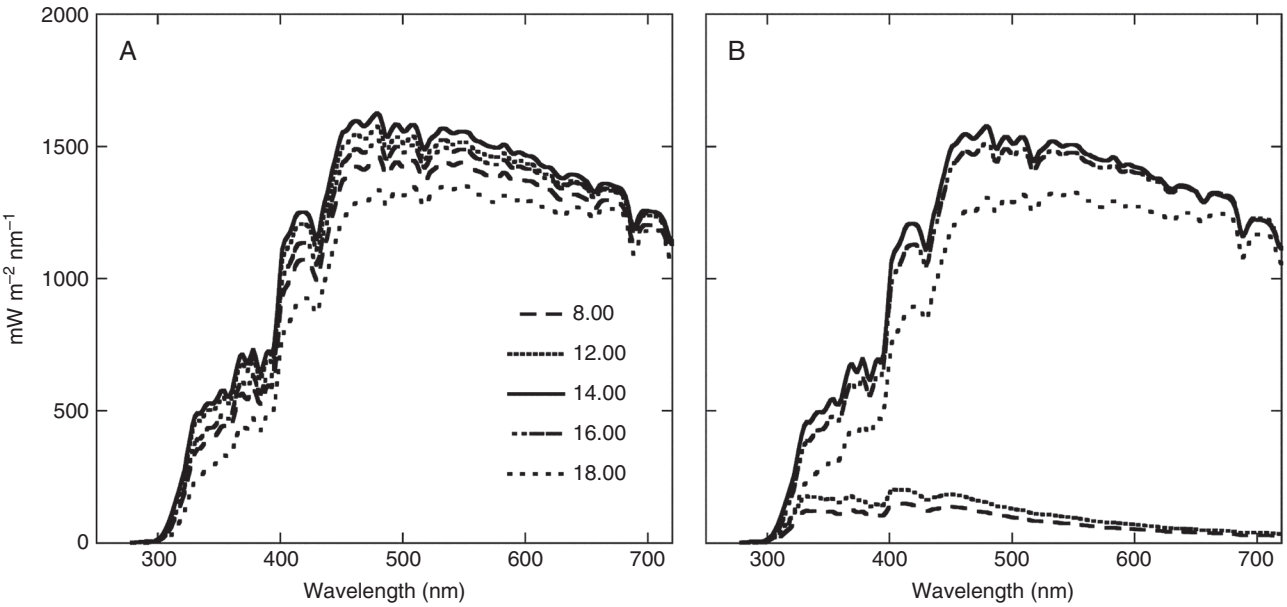

FIG. 5. Change in sunlight spectra in Antarctic habitats during one sunny day. (A) Instantaneous sunlight spectral patterns were measured by a spectrophotometer at the open site and (B) in the *P. crispa* habitat on 2 January 2013. It was a clear fine day.

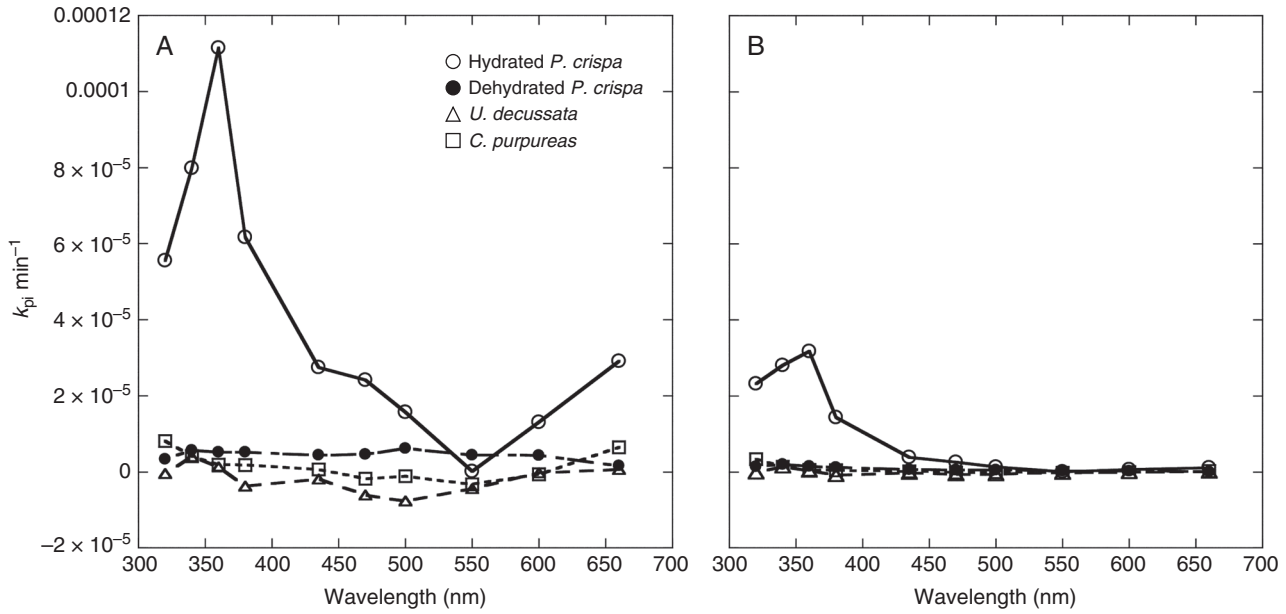

FIG. 6. Wavelength dependency of the rate constant, k_{pi}, of photoinactivation against irradiation under ambient sunlight conditions in *P. crispa*, *U. decussata* and *C. purpureus*. Rate constants of photoinactivation were calculated at the open site (A) and near the *P. crispa* habitat (B) at 12.00 h when the site was shaded by a rock.

constant of recovery, k_{rec}, at the site is needed. However, determination of the rate constant under natural conditions is not easy because the activity of the repair system depends on many factors such as light intensity, temperature and water content. In order to estimate k_{rec}, we compared F_v/F_m as a function of time between streptomycin-treated and non-treated samples by a solar simulator HAL-C100 (Asahi Spectra, Tokyo, Japan) for fully hydrated samples at the optimal temperature (15 °C) of photosynthesis. In a fully hydrated sample which was treated with streptomycin to inhibit the repair system, F_v/F_m decreased exponentially with time (Fig. 9, filled circles with solid line). The decline was reproduced well by calculated k_{pi}s obtained by summation of $\left(E_{pi}\right)_\lambda \times I_\lambda$ under three different light intensities (Fig. 9, crosses with broken line). The results indicate that the calculated k_{pi} reflects the time course of decline of PSII (F_v/F_m) well. We can thus estimate the rate constants of recovery, k_{rec}s, from the time course of F_v/F_m (Fig. 9, open circles with solid line) in the absence of streptomycin and the calculated k_{pi} by the following equation (Wünschmann and Brand, 1992).

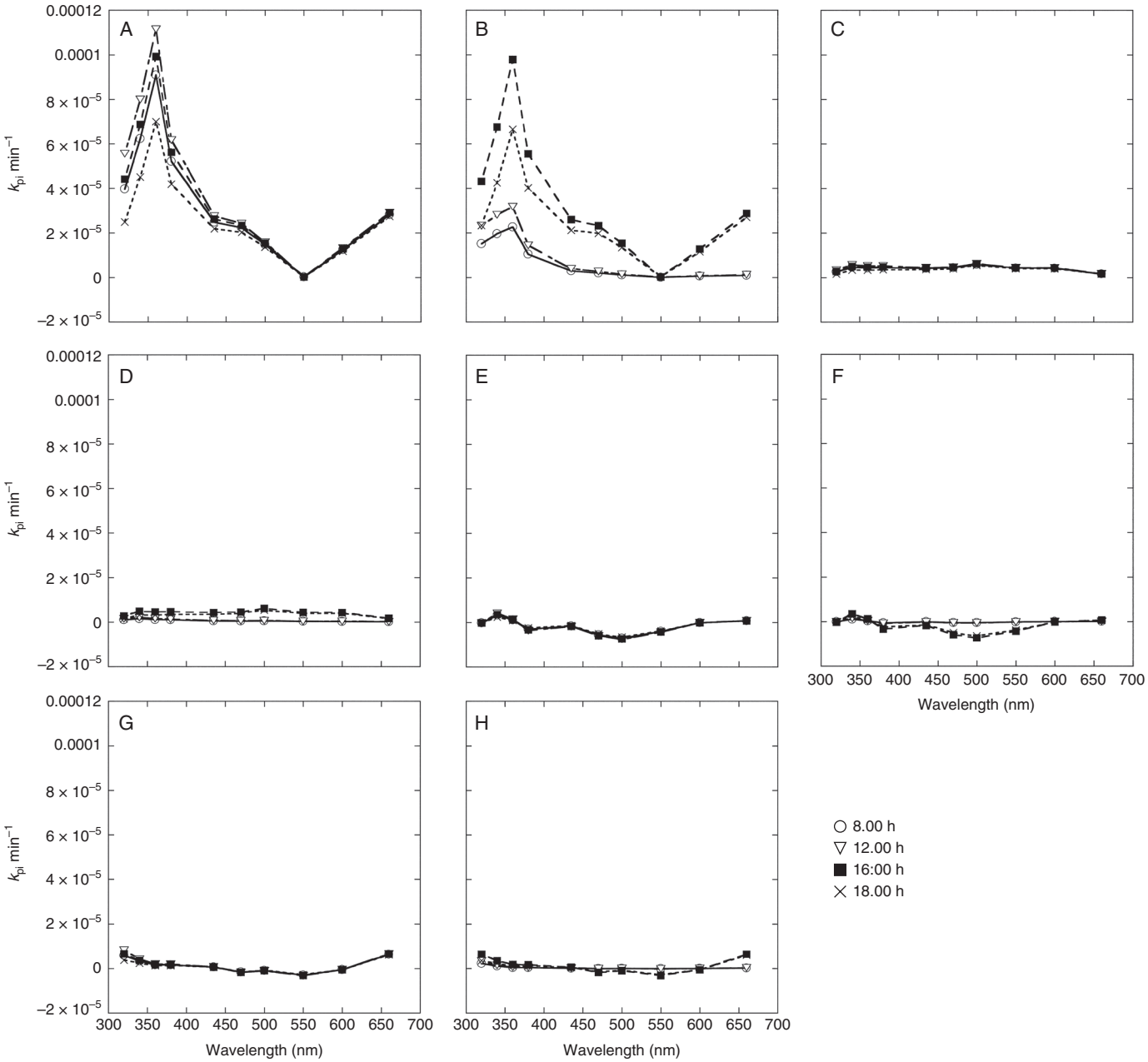

FIG. 7. Daily variation in wavelength dependency of the rate constant, k_{pi}, of photoinactivation against irradiation at ambient sunlight conditions in *P. crispa*, *U. decussate* and *C. purpureus*. Rate constants of photoinactivation were calculated in hydrated *P. crispa* (A, B), dehydrated *P. crispa* (C, D), *U. decussate* (E, F) and *C. purpureus* (G, H) at the open site (A, C, E, G) and near the *P. crispa* habitat on a sunny day (2 January 2 2013).

$$y = \left\{ k_{rec} + k_{\mathrm{pi}} \times \frac{e^{\left[\left(k_{pi}+k_{rec}\right)\times t\right]}}{\left(k_{rec}+k_{pi}\right)} \right\} \qquad (12)$$

The energy doses used for the calculation of Fig. 9 are shown in Table 2. The k_{rec}s calculated from eqn (12) were 0.026, 0.062 and 0.033 (min^{-1}) at 260, 580 and 1750 µmol photons m^{-2} s^{-1}, respectively. Assuming that k_{rec} is constant under the same light conditions, y (F_v/F_m) is calculated to reach a stationary level of 0.85, 0.88 and 0.66 at 260, 580 and 1750 µmol photons m^{-2} s^{-1}, respectively. We can thus calculate a repair cost, C_{Photo}, from the rate constant of recovery, k_{rec}, the repair cost per PSII unit, C_{PSII}, and the number of PSII units per unit area, $\mathrm{D1}_{\mathrm{area}}$ (Miyata *et al.*, 2012):

$$C_{\mathrm{Photo}} = \left(1 - y\right) k_{\mathrm{rec}} \times C_{\mathrm{PSII}} \times \mathrm{D1}_{\mathrm{area}} \qquad (13)$$

The $(1 - y)$ k_{rec} vlaues per minute were calculated to be 0.0038, 0.0073 and 0.0110 for 260, 580 and 1750 µmol photons m^{-2} s^{-1} of white light, respectively. The obtained values suggested that PSII in *P. crispa* will be able to keep about 85 % of full activity at 580 µmol photons m^{-2} s^{-1} of sunlight irradiation by paying twice the cost for restoration of damaged PSII

than at 260 μmol photons m^{-2} s^{-1}. Under higher intensities such as direct sunlight during the summer, however, photosynthetic efficiency will decline because of the low k_{rec} value.

In dehydrated conditions, photoinactivation damage is accumulated as long as the photosynthetic organisms are kept in a dehydrated condition, because all metabolism, including the repair cycle of photosystems, stops in the absence of water. After rehydration, the accumulated photodamage induces photoinhibition, i.e. photoinactivation in a dehydrated condition is directly connected to photoinhibition, so the accumulated fraction of photoinhibition is defined as $1-a\times e^{k_{pi}\times t}$ [eqn (5)]. The photoinhibition induced by UV radiation was suppressed to nearly zero for dehydrated *P. crispa*. Figure 10 shows the accumulated photodamage in dehydrated *P. crispa* during the day (08.00–18.00 h) in the open site and the natural habitat estimated from the sun spectral data and rate constants, k_{pi}. The accumulated photodamage in PSII for the dehydrated thalli was estimated to reach 65 and 43 % in the open site and the natural habitat, respectively.

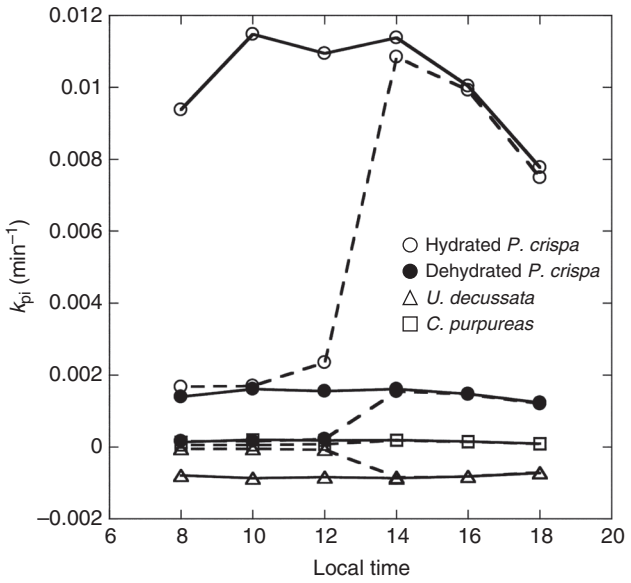

FIG. 8. Temporal changes in the rate constants of photoinactivation in PSII in *P. crispa*, *U. decussata* and *C. purpureus* in their habitats on a sunny summer day in Antarctica. Rate constants of photoinactivation in PSII at the habitats were calculated as $k_{pi}=\sum_{320\,nm}^{660\,nm}\left\{\left(E_{pi}\right)_{\lambda}\times I_{\lambda}\right\}(min^{-1})$ at the open site (solid line) and near the *P. crispa* habitat (dashed line).

DISCUSSION

In the present study, wavelength dependency of photoinactivation for photosynthetic organisms growing in continental Antarctica was compared by measuring the reaction coefficients of inactivation of PSII in monochromatic light in order to elucidate environmental factors which induce photoinhibition. A green alga, *P. crispa*, was found to be fairly sensitive to UV light (Table 1; Fig. 4). High reaction coefficients have been reported in many vascular and non-vascular plants against wavelengths shorter than blue light (Tyystjärvi *et al.*, 2002; Sarvikas *et al.*, 2006; Hakala-Yatkin *et al.*, 2010). The inactivation process induced by short wavelength light corresponds to OEC degradation, whereas long wavelengths scarcely affect the OEC (Durrant *et al.*, 1990; Ohnishi *et al.*, 2005). Kok *et al.* (1966) indicated that absorption of light energy by antenna chlorophylls is correlated with photoinactivation, and concluded that photoinactivation by red light takes place as a result of energy absorption by chlorophyll. It has been suggested that red light induces photoinactivation by producing ROS in photochemical reactions (Santabarbara *et al.*, 2001; Krieger-Liszkay *et al.*, 2008, Vass, 2011). However, it was found that ROS rarely destroy PSII but inhibit recovery of damaged PSII (Nishiyama *et al.*, 2004; Murata *et al.*, 2007). Moreover, direct

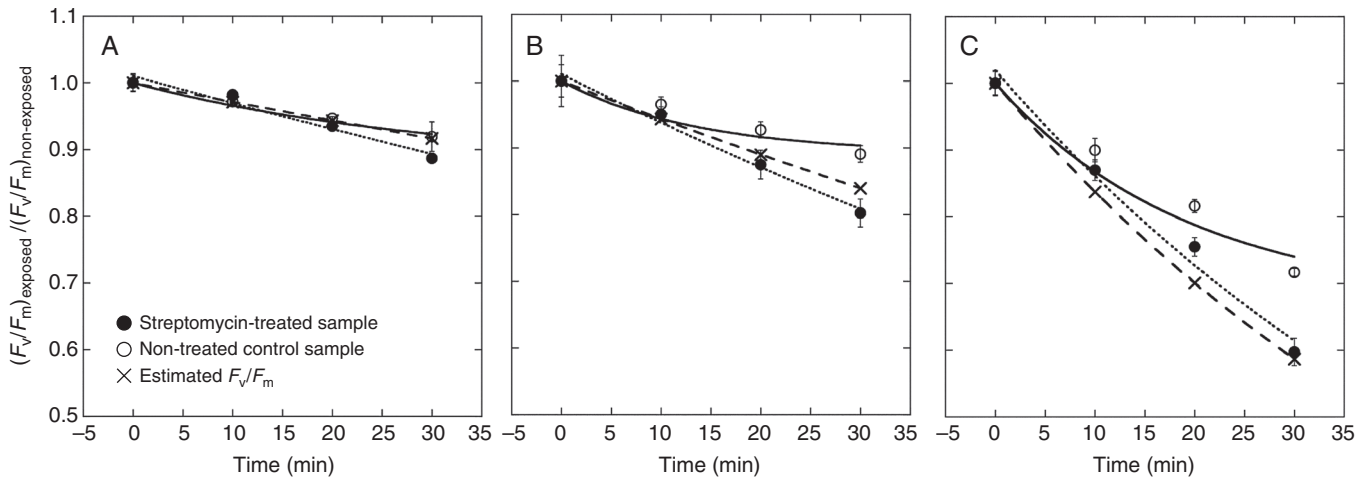

FIG. 9. Decrease in PSII quantum yield under three different light intensities illuminated by artificial sunlight. Maximum PSII quantum yields of *P. crispa* thalli after irradiation by a solar simulator were measured against duration of irradiation. The light intensities were set to 260 (A), 580 (B) and 1750 (C) μmol photons m^{-2} s^{-1}. Filled circles and open circles indicate the yields of the streptomycin-treated and non-treated (control) sample, respectively. Crosses show estimated F_v/F_m calculated from the rate constant, k_{pi}, obtained by $\sum_{320\,nm}^{660\,nm}\left\{\left(E_{pi}\right)_{\lambda}\times I_{\lambda}\right\}(min^{-1})$.

damaging processes in PSII by ROS have been demonstrated in many studies, and photoinactivation by red light was observed *in vivo* for several higher plants and a diatom (Oguchi *et al.*, 2009; Zavafer *et al.*, 2015; Havurinne and Tyystjärvi, 2017). In this study, we confirmed the effects of red light on fluorescence yield decline of PSII of *P. crispa* in the presence of a protein synthesis inhibitor by which the PSII recovery process is suppressed. A small peak at 660 nm of the reaction coefficient, E_{pi}, plotted against irradiation dose was found in Fig. 4, but the magnitude of the rate constant, k_{pi}, at 660 nm against a sunlight spectrum at noon in the habitat was rather large because of the high amount of the red light component relative to that of UV (Fig. 6A). Effects of insufficient relaxation of non-photochemical fluorescence quenching, which induces a decrease in fluorescence intensity and fluorescence yield, can be ruled out because the samples used were kept in the dark for >30 min before fluorescence measurements.

The difference in wavelength dependency of photoinactivation among the samples used in the present study appears to be derived from the difference in shielding mechanisms of irradiated light in each organism. Small E_{pi} values observed at wavelengths between 320 and 750 nm for *U. decussata* and *C. purpureus* indicated that protection mechanisms from absorbing hazardous irradiation are functioning well to avoid photoinhibition. Lichens are highly tolerant to UV radiation by scattering UV light at the upper cortex, which consists of fungal hyphae, and by the presence of several UV-absorbing substances in their thalli (Dietz *et al.*, 2000; Nybakken *et al.*, 2004; Kosugi *et al.*, 2010*b*). We have confirmed in this study that the Antarctic bryophyte *C. purpureus* predominantly had sensitivity to UV-B but not to UV-A radiation (320 nm) (Fig. 2) (Green et.al, 2005; Turnbull and Robinson, 2009). *Ceratodon purpureus* also accumulates UV-absorbing substances in its cell walls, acting as a shield for UV light. The organism is highly tolerant to UV radiation (Clarke and Robinson, 2008)

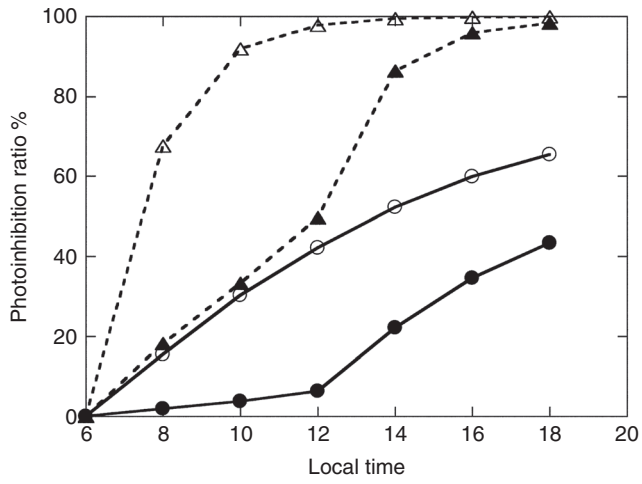

FIG. 10. Estimation of accumulation of photoinactivated PSII in dehydrated *P. crispa* in its habitat on a sunny summer day in Antarctica. The photoinactivation ratio in dehydrated *P. crispa* in the open site and in its habitat (closed circles, solid line) on a summer day was estimated by using the equation (photoinactivation ratio) = $1-a\times e^{-E_{pi}\times I\times t}(=1-a\times e^{-k_{pi}\times t})$, with reaction coefficients, E_{pi}s, in a dehydrated condition (solid lines) or a hydrated condition (dotted lines).

due to these substances. Although *P. crispa* contains some UV-absorbing substances, such as MAAs that show an absorption peak at around 320 nm (Hoyer *et al.*, 2001), this was not sufficient to prevent photoinactivation. Despite the difference in wavelength dependency of photoinactivation among the three species tested, they can all form large colonies and are often dominant photosynthetic terrestrial organisms in the ice-free oases of Antarctica. Our observations suggest that the species adopt different adaptation strategies against light stresses in their natural habitat. In this study, we focused on the inactivation process of PSII by irradiation in the presence of a protein synthesis inhibitor, streptomycin, to avoid mixed effects by the repair cycle.

Under natural conditions, the observed PSII activity reflects a result of a balance between its degradation and recovery rate. In fact, the F_v/F_m of *P. crispa* measured in an Antarctic maritime habitat was almost constant during the day. It should be noted that the environmental conditions of a maritime habitat are milder than those of the continental surface of Antarctica (Lud *et al.*, 2001). Even when PSII is damaged in the daytime, the damage is fully recovered during the evening and at night (Lud *et al.*, 2001). These findings indicate that the PSII repair cycle in this species has enough capacity to maintain PSII function under such low-temperature conditions. When PSII is damaged, PSII proteins, such as D1, D2, CP43 and CP47, enter rapidly into the repair cycle (Yamamoto and Akasaka, 1995; Jansen *et al.*, 1999; Ma *et al.*, 2007). In order to maintain PSII activity, the PSII complex should be reconstructed. However, energy is needed for degradation of inactivated PSII and reconstruction of the complex. The cost and benefit of repair have been calculated in some reports (Raven and Samuelsson, 1986; Raven, 1989; Miyata *et al.*, 2012). Miyata *et al.* (2012) indicated that close to 2 % of total ATP synthesized by the photochemical reaction is needed for restoration of activated PSII in spinach. They irradiated spinach with a halogen lamp which emits light longer than 400 nm, and estimated the k_{pi} value assuming that it is constant under any wavelengths of the PAR range.

We have estimated a rate constant, k_{pi}, in a visible light region for hydrated *P. crispa* at the open site at 12.00 h by using the calculated E_{pi} values of each wavelength. The average PAR intensity per hour after 12.00 h near the habitat was estimated to be 1620 µmol photons m^{-2} s^{-1} on 2 January (Kudoh *et al.*, 2015*b*). The value obtained was $\sum_{380\,nm}^{660\,nm}\left\{\left(E_{pi}\right)_{\lambda}\times I_{\lambda}\right\}=0.006\,min^{-1}$ (the k_{pi} values at 320–380 nm were excluded) in *P. crispa.* This is very close to the value (k_{pi} = 0.005–0.007 min^{-1}) of Miyata *et al.* (2012) for spinach irradiated at 1600 µmol photons m^{-2} s^{-1}. This suggests that the sensitivity of PSII to irradiation is quite similar between *P. crispa* and spinach.

We demonstrated that it was possible to reproduce the photoinactivation rate under artificial sunlight by using E_{pi} at each wavelength. The observed values measured in the presence of streptomycin coincided well with estimated values calculated by eqn (5). It was indicated that the repair rate depended on the photoinactivation in a range of weak light intensities in *Synechocystis* 6803 (Wünschmann and Brand, 1992; Allakhverdiev and Murata, 2004). In our study, the highest k_{rec} was observed at 580 µmol photons m^{-2} s^{-1} and it was larger than the maximum value observed in spinach (Miyata *et al.*, 2012), and the electron transport rate

(ETR) was close to maximum at around 500 µmol photons m^{-2} s^{-1} in *P. crispa* (Kosugi *et al.*, 2010*a*). It could be concluded that high photosynthetic efficiency is achieved at 500 µmol photons m^{-2} s^{-1} irradiation in *P. crispa*.

Costs which are necessary to be paid to recover photoinactivation increase with increasing light intensity in photosynthetic organisms. In the case of higher plants, k_{rec} increases with increasing light intensity and reaches a constant value (Miyata *et al.*, 2012). However, PSII activity of *P. crispa* decreased to 66 % in the high light condition, at 1750 µmol m^{-2} s^{-1}, because of the k_{rec} becoming smaller than that at 580 µmol m^{-2} s^{-1}. It was possible that the repair cycle was damaged during illumination or limited for some reason. The light condition of 1750 µmol m^{-2} s^{-1} obtained by artificial sunlight is close to the maximum irradiation of direct sunlight at the habitat during the summer. When the recovery rate becomes lower than the degradation rate of PSII proteins, a critical energy loss would occur because of a decrease in the CO_2 fixation rate (Miyata *et al.*, 2012). A decline of k_{rec} and an increase of the repair cost under high light intensity must increase the photoinhibition risk in *P. crispa* after melting snow in the habitat during the summer season.

Umbilicaria decussata and *C. purpureus* could avoid high costs for the recovery from photodamage since they were resistant to photoinactivation (Figs 6 and 8). The two organisms show negative E_{pi} values at some tested wavelengths, although these E_{pi} values are almost zero. A small number of the measurements (d.f. = 5) is one of the causes of statistical uncertainty in E_{pi} in the two organisms. They can retain high photosynthetic capacity of PSII in a wide range of light intensities. Alternatively, the two species put more energy into protection against photoinactivation, rather than for machinery to recover from photoinactivation. Judging from the k_{pi} values, it is clear that *U. decussata* and *C. purpureus* had much higher tolerance to photoinactivation than higher plants. Because the chlorophyll content per unit area in *C. purpureus* is larger by about 1.5-fold than that of the other tested species, as described in the Materials and Methods, the amount of PSII per unit area (amount of D1) might be larger and the repair cost per unit time larger than for the other species. However, even after taking into consideration the above, it is clear that hydrated *P. crispa* need several times more energy to maintain photosynthetic activity compared with the lichen and the bryophyte in the open site.

Wavelength dependency of photoinactivation under dehydrated conditions for drought-tolerant photosynthetic organisms has not been reported so far. We have shown that *P. crispa* possesses characteristic features of d-NPQ that are widely observed for drought-tolerant poikilohydric organisms (Komura *et al.*, 2010; Kosugi *et al.*, 2010*a*). Drought tolerance would prevent photoinhibition through a d-NPQ mechanism in which absorbed energy by chlorophylls is dissipated as heat, as was clear by the suppression of E_{pi} values in the red and blue light regions under drought conditions (Fig. 4). It should be noted that *P. crispa* is rather tolerant to VIS and UV irradiation in its dehydrated form. The E_{pi} values for the dehydrated state dropped to one-tenth of those of the hydrated samples. In other words, photoinactivation caused by OEC disruption is extremely suppressed under drought conditions. An increase in the fraction of reflectance in dehydrated cells will result in a decrease of penetration of UV radiation reaching the OEC. However, dehydrated thalli of *P. crispa* do not show a change in the absorption spectral form compared with the hydrated condition (data not shown). It is possible that the relative concentration of UV-absorbing substances becomes high in dehydrated cells and they protect the OEC from UV radiation. Another possible explanation is the increasing stabilization of the OEC under drought conditions. Although the mechanism is still unclear, an increase in OEC stability under drought conditions has been demonstrated by heat treatment of dehydrated *Nostoc commune*, the terrestrial cyanobacterium (Fukuda *et al.*, 2008). It is important to note that the risk of photoinhibition by irradiation with both the VIS and UV spectral regions decreases enormously under drought conditions. This would be an adaptive advantage for *P. crispa*. It is often exposed to strong sunlight for long periods after the snow cover disappears in late summer. If these protection mechanisms were not functioning, *P. crispa* would accumulate large amounts of photodamage as it dries out because the repair cycle would not be functioning. It would lead to a significant decrease of photosynthetic activity after rehydration. If the drought-induced protection mechanisms did not operate properly, the PSII quantum yield would drop to <5 % within 1 d at the habitat (Fig. 10). This suggests that the dehydrated form is advantageous for suppressing photoinactivation of *P. crispa*.

Our results clearly demonstrated that *P. crispa* has needed to depend on the ability of recover in order to keep the PSII working to its full extent, whereas the lichen and bryophyte use different tactics to protect against disruption of the photosystem. A variety of strategies against photoinhibition exist in dominant species of Antarctica, depending on the organism's ecology.

ACKNOWLEDGEMENTS

We thank all members of the Japan Antarctic Research Expedition (JARE) 54 and JARE 55 for their support, the captain and crew of the icebreaker *Shirase*, and Mr. Shoichi Higashi and Mr Tamaki Uchikawa for use of the large spectrograph. This study was supported by the Japan Society for the Promotion of Science (24770030), the Sumitomo Foundation (151376), NIPR Project Research (KP-8) and the NIBB Collaborative Research Program for the Okazaki Large Spectrograph (13–504, 14–503 to M.K.). The production of this paper was supported by an NIPR publication subsidy.

LITERATURE CITED

Allakhverdiev SI, **Murata N. 2004**. Environmental stress inhibits the synthesis de novo of proteins involved in the photodamage–repair cycle of Photosystem II in *Synechocystis* sp. PCC 6803. *Biochimica et Biophysica Acta* **1657**: 23–32.

Aro EM, **Virgin I**, **Andersson B. 1993**. Photoinhibition of Photosystem II. Inactivation, protein damage and turnover. *Biochimica et Biophysica Acta* **1143**: 113–134.

Asada K. 1999. The water–water cycle in chloroplasts: scavenging of active oxygens and dissipation of excess photons. *Annual Review of Plant Physiology and Plant Molecular Biology* **50**: 601–639.

Asada K, **Heber U**, **Schreiber U. 1992**. Pool size of electrons that can be donated to $P700^+$ as determined in intact leaves: donation to $P700^+$ from stromal components via the intersystem chain. *Plant and Cell Physiology* **33**: 927–932.

Asada K, **Heber U**, **Schreiber U. 1993**. Electron flow to the intersystem chain from stromal components and cyclic electron flow in maize chloroplasts,

as detected in intact leaves by monitoring redox change of P700 and chlorophyll fluorescence. *Plant and Cell Physiology* **34**: 39–50.

Bondarava N, **Gross CM**, **Mubarakshina M**, **Golecki JR**, **Johnson GN**, **Krieger-Liszkay A. 2010**. Putative function of cytochrome b559 as a plastoquinol oxidase. *Physiologia Plantarum* **138**: 463–473.

Campbell DA, **Tyystjarvi E. 2012**. Parameterization of photosystem II photoinactivation and repair. *Biochimica et Biophysica Acta* **1817**: 258–265.

Clarke LJ, **Robinson SA. 2008**. Cell wall-bound ultraviolet-screening compounds explain the high ultraviolet tolerance of the Antarctic moss, *Ceratodon purpureus*. *New Phytologist* **179**: 776–783.

Dietz S, **Budel B**, **Lange OL**, **Bilger W. 2000**. Transmittance of light through the cortex of lichens from contrasting habitats. *Bibliotheca Lichenologica* **75**: 171–182.

Ding S, **Jiang R**, **Lu Q**, **Wen X**, **Lu C. 2016**. Glutathione reductase 2 maintains the function of photosystem II in *Arabidopsis* under excess light. *Biochimica et Biophysica Acta* **1857**: 665–677.

Durrant JR, **Giorgi LB**, **Barber J**, **Klug DR**, **Porter G. 1990**. Characterisation of triplet states in isolated Photosystem II reaction centres: oxygen quenching as a mechanism for photodamage. *Biochimica et Biophysica Acta* **1017**: 167–175.

Fukuda SY, **Yamakawa R**, **Hirai M**, **Kashino Y**, **Koike H**, **Satoh K. 2008**. Mechanisms to avoid photoinhibition in a desiccation-tolerant cyanobacterium, *Nostoc commune*. *Plant and Cell Physiology* **49**: 488–492.

Green TGA, **Kulle D**, **Pannewitz S**, **Sancho LG**, **Schroeter B. 2005**. UV-A protection in mosses growing in continental Antarctica. *Polar Biology* **28**: 822–827.

Hakala-Yatkin M, **Tyystjärvi E. 2011**. Inhibition of Photosystem II by the singlet oxygen sensor compounds TEMP and TEMPD. *Biochimica et Biophysica Acta* **1807**: 243–250.

Hakala M, **Tuominen I**, **Keranen M**, **Tyystjärvi T**, **Tyystjärvi E. 2005**. Evidence for the role of the oxygen-evolving manganese complex in photoinhibition of Photosystem II. *Biochimica et Biophysica Acta* **1706**: 68–80.

Hakala M, **Rantamaki S**, **Puputti EM**, **Tyystjärvi T**, **Tyystjärvi E. 2006**. Photoinhibition of manganese enzymes: insights into the mechanism of photosystem II photoinhibition. *Journal of Experimental Botany* **57**: 1809–1816.

Hakala-Yatkin M, **Mantysaari M**, **Mattila H**, **Tyystjärvi E. 2010**. Contributions of visible and ultraviolet parts of sunlight to photoinhibition. *Plant and Cell Physiology* **51**: 1745–1753.

Havurinne V, **Tyystjärvi E. 2017**. Action spectrum of photoinhibition in the diatom *Phaeodactylum tricornutum*. *Plant and Cell Physiology* **58**: 2217–2225.

Heber U, **Lange OL**, **Shuvalov VA. 2006**. Conservation and dissipation of light energy as complementary processes: homoiohydric and poikilohydric autotrophs. *Journal of Experimental Botany* **57**: 1211–1223.

Hideg E, **Kós PB**, **Vass I. 2016**. Photosystem II damage induced by chemically generated singlet oxygen in tobacco leaves. *Physiologia Plantarum* **131**: 33–40.

Hirai M, **Yamakawa R**, **Nishio J**, ***et al.* 2004**. Deactivation of photosynthetic activities is triggered by loss of a small amount of water in a desiccation-tolerant cyanobacterium, *Nostoc commune*. *Plant and Cell Physiology* **45**: 872–888.

Hoyer K, **Karsten U**, **Sawall T**, **Wiencke C. 2001**. Photoprotective substances in Antarctic macroalgae and their variation with respect to depth distribution, different tissues and developmental stages. *Marine Ecology Progress Series* **211**: 117–129.

Jansen MA, **Mattoo AK**, **Edelman M. 1999**. D1-D2 protein degradation in the chloroplast. Complex light saturation kinetics. *European Journal of Biochemistry* **260**: 527–532.

Jones LW, **Kok B. 1966**. Photoinhibition of chloroplast reactions. I. Kinetics and action spectra. *Plant Physiology* **41**: 1037–1043.

Jung J, **Kim HS. 1990**. The chromophores as endogenous sensitizers involved in the photogeneration of singlet oxygen in spinach thylakoids. *Photochemistry and Photobiology* **52**: 1003–1009.

Kanda H, **Inoue M. 1994**. Ecological monitoring of moss and lichen vegetation in the syowa station area, Antarctica (15th Symposium on Polar Biology). *Proceedings of the NIPR Symposium on Polar Biology* **7**: 221–231.

Kok B. 1956. On the inhibition of photosynthesis by intense light. *Biochimica et Biophysica Acta* **21**: 234–244.

Kok B, **Gassner EB**, **Rurainski HJ. 1966**. Photoinhibition of chloroplast reactions. *Photochemistry and Photobiology* **4**: 215–227.

Komura M, **Yamagishi A**, **Shibata Y**, **Iwasaki I**, **Itoh S. 2010**. Mechanism of strong quenching of photosystem II chlorophyll fluorescence under drought stress in a lichen, *Physciella melanchla*, studied by subpicosecond fluorescence spectroscopy. *Biochimica et Biophysica Acta* **1797**: 331–338

Kondratyev KY. 1969. *Radiation in the atmosphere. International Geophysics Series 12*. London: Academic Press.

Kosugi M, **Arita M**, **Shizuma R**, ***et al.* 2009**. Responses to desiccation stress in lichens are different from those in their photobionts. *Plant and Cell Physiology* **50**: 879–888.

Kosugi M, **Katashima Y**, **Aikawa S**, ***et al.* 2010*a***. Comparative study on the photosynthetic properties of *Prasiola* (chlorophyceae) and *Nostoc* (cyanophyceae) from Antarctic and non-Antarctic sites. *Journal of Phycology* **46**: 466–476.

Kosugi M, **Yasuhiro K**, **Satoh K. 2010*b***. Comparative analysis of light response curves of *Ramalina yasudae* and freshly isolated *Trebouxia* sp. revealed the presence of intrinsic protection mechanisms independent of upper cortex for the photosynthetic system of algal symbionts in lichen. *Lichenology* **9**: 1–10.

Kosugi M, **Kurosawa N**, **Kawamata A**, **Kudoh S**, **Imura S. 2015**. Year-round micrometeorological data from the habitats of terrestrial photosynthetic organisms in Langhovde, East Antarctica, during 2013. *JARE Data Reports. Terrestrial Biology* **8**: 1–6.

Krause GH, **Weis E. 1991**. Chlorophyll fluorescence and photosynthesis: the basics. *Annual Review of Plant Physiology and Plant Molecular Biology* **42**: 313–349.

Krieger-Liszkay A, **Fufezan C**, **Trebst A. 2008**. Singlet oxygen production in photosystem II and related protection mechanism. *Photosynthesis Research* **98**: 551–564.

Kudoh H, **Sonoike K. 2002**. Irreversible damage to photosystem I by chilling in the light: cause of the degradation of chlorophyll after returning to normal growth temperature. *Planta* **215**: 541–548

Kudoh S, **Takahashi K**, **Ishihara T**, ***et al.* 2015*a***. Meteorological data from ice-free areas in Yukidori Zawa, Langhovde, Kizahashi Hama, Skarvsnes and Skallen in Sôya Coast, East Antarctica during 2014–2015. *JARE Data Reports. Terrestrial Biology* **11**: 1–6.

Kudoh S, **Tanabe Y**, **Uchida M**, **Imura S. 2015*b***. Meteorological data from ice-free areas in Yukidori Zawa, Langhovde and Kizahashi Hama, Skarvsnes in Sôya Coast, East Antarctica during 2009–2014. *JARE Data Reports. Terrestrial Biology* **9**: 1–7.

Kurreck J, **Schödel RE**, **Renger G. 2000**. Investigation of the plastoquinone pool size and fluorescence quenching in thylakoid membranes and Photosystem II (PS II) membrane fragments. *Photosynthesis Research* **63**: 171–182.

Long SP, **Humphries S**, **Falkowski PG. 1994**. Photoinhibition of photosynthesis in nature. *Annual Review of Plant Physiology and Plant Molecular Biology* **45**: 633–662.

Longton RE. 1988. Adaptations and strategies of polar bryophytes. *Botanical Journal of the Linnean Socie* **98**: 253–268.

Lud D, **Buma AGJ**, **Van De Poll W**, **Moerdijk TCW**, **Huiskes AHL. 2001**. DNA damage and photosynthetic performance in the Antarctic terrestrial alga *Prasiola crispa* ssp. Antarctica (chlorophyta) under manipulated UV-B radiation. *Journal of Phycology* **37**: 459–467.

Ma J, **Peng L**, **Guo J**, **Lu Q**, **Lu C**, **Zhang L. 2007**. LPA2 is required for efficient assembly of photosystem II in *Arabidopsis thaliana*. *The Plant Cell* **19**: 1980–1993.

Melis A. 1999. Photosystem-II damage and repair cycle in chloroplasts: what modulates the rate of photodamage *in vivo*? *Trends in Plant Science* **4**: 130–135.

Miyata K, **Noguchi K**, **Terashima I. 2012**. Cost and benefit of the repair of photodamaged photosystem II in spinach leaves: roles of acclimation to growth light. *Photosynthesis Research* **113**: 165–180.

Murata N, **Takahashi S**, **Nishiyama Y**, **Allakhverdiev SI. 2007**. Photoinhibition of photosystem II under environmental stress. *Biochimica et Biophysica Acta* **1767**: 414–421.

Nabe H, **Funabiki R**, **Kashino Y**, **Koike H**, **Satoh K. 2007**. Responses to desiccation stress in bryophytes and an important role of dithiothreitol-insensitive nonphotochemical quenching against photoinhibition in dehydrated states. *Plant and Cell Physiology* **48**: 1548–1557.

Nishiyama Y, **Yamamoto H**, **Allakhverdiev SI**, **Inaba M**, **Yokota A**, **Murata N. 2001**. Oxidative stress inhibits the repair of photodamage to the photosynthetic machinery. *EMBO Journal* **20**: 5587–5594.

Nishiyama Y, **Allakhverdiev SI**, **Yamamoto H**, **Hayashi H**, **Murata N. 2004**. Singlet oxygen inhibits the repair of photosystem II by suppressing the translation elongation of the D1 protein in *Synechocystis* sp. PCC 6803. *Biochemistry* **43**: 11321–1130.

Nishiyama Y, **Allakhverdiev SI**, **Murata N. 2006**. A new paradigm for the action of reactive oxygen species in the photoinhibition of photosystem II. *Biochimica et Biophysica Acta* **1757**: 742–749.

Nybakken L, **Solhaug KA**, **Bilger W**, **Gauslaa Y. 2004**. The lichens *Xanthoria elegans* and *Cetraria islandica* maintain a high protection against UV-B radiation in Arctic habitats. *Oecologia* **140**: 211–216.

Oguchi R, **Terashima I**, **Chow WS. 2009**. The involvement of dual mechanisms of photoinactivation of photosystem II in *Capsicum annuum* L. plants. *Plant and Cell Physiology* **50**: 1815–1825.

Ohnishi N, **Allakhverdiev SI**, **Takahashi S**, ***et al.*** **2005**. Two-step mechanism of photodamage to photosystem II: step 1 occurs at the oxygen-evolving complex and step 2 occurs at the photochemical reaction center. *Biochemistry* **44**: 8494–8499.

Porra RJ, **Thompson WA**, **Kriedemann PE. 1989**. Determination of accurate extinction coefficients and simultaneous equations for assaying chlorophylls *a* and *b* extracted with four different solvents: verification of the concentration of chlorophyll standards by atomic absorption spectroscopy. *Biochimica et Biophysica Acta* **975**: 384–394.

Powles SB. 1984. Photoinhibition of photosynthesis induced by visible light. *Annual Review of Plant Physiology* **35**: 15–44.

Raven JA. 1989. Flight or flight: the economics of repair and avoidance of photoinhibition of photosynthesis. *Functional Ecology* **3**: 5–19.

Raven JA, **Samuelsson G. 1986**. Repair of photoinhibitory damage in anacystis nidulans 625 (*Synechococcus* 6301): relation to catalytic capacity for, and energy supply to, protein synthesis, and implications for μ_{max} and the efficiency of light-limited growth. *New Phytologist* **103**: 625–643.

Rozema J, **Björn LO**, **Bornman JF**, ***et al.*** **2002**. The role of UV-B radiation in aquatic and terrestrial ecosystems – an experimental and functional analysis of the evolution of UV-absorbing compounds. *Journal of Photochemistry and Photobiology B: Biology* **66**: 2–12.

Santabarbara S, **Neverov KV**, **Garlaschi FM**, **Zucchelli G**, **Jennings RC. 2001**. Involvement of uncoupled antenna chlorophylls in photoinhibition in thylakoids. *FEBS Letters* **491**: 109–113.

Sarvikas P, **Hakala M**, **Patsikka E**, **Tyystjärvi T**, **Tyystjärvi E. 2006**. Action spectrum of photoinhibition in leaves of wild type and *npq1-2* and *npq4-1* mutants of *Arabidopsis thaliana*. *Plant and Cell Physiology* **47**: 391–400.

Schnettger B, **Critchley C**, **Santore UJ**, **Graf M**, **Krause GH. 1994**. Relationship between photoinhibition of photosynthesis, D1 protein turnover and chloroplast structure: effects of protein synthesis inhibitors. *Plant, Cell and Environment* **17**: 55–64.

Sonoike K. 2011. Photoinhibition of photosystem I. *Physiologia Plantarum* **142**: 56–64.

Sonoike K, **Terashima I**, **Iwaki M**, **Itoh S. 1995**. Destruction of photosystem I iron–sulfur centers in leaves of *Cucumis sativus* L. by weak illumination at chilling temperatures. *FEBS Letters* **362**: 235–238.

Takahashi M, **Asada K. 1988**. Superoxide production in aprotic interior of chloroplast thylakoids. *Archives of Biochemistry and Biophysics* **267**: 714–722

Takahashi S, **Murata N. 2008**. How do environmental stresses accelerate photoinhibition? *Trends in Plant Science* **13**: 178–182.

Terashima I, **Funayama S**, **Sonoike K. 1994**. The site of photoinhibition in leaves of *Cucumis sativus* L. at low temperatures is photosystem I, not photosystem II. *Planta* **193**: 300–306.

Turnbull JD, **Robinson SA. 2009**. Accumulation of DNA damage in Antarctic mosses: correlations with ultraviolet-B radiation, temperature and turf water content vary amongst species. *Global Change Biology* **15**: 319–329.

Tyystjärvi E. 2013. Photoinhibition of Photosystem II. *International Review of Cell and Molecular Biology* **300**: 243–303.

Tyystjärvi E, **Aro EM. 1996**. The rate constant of photoinhibition, measured in lincomycin-treated leaves, is directly proportional to light intensity. *Proceedings of the National Academy of Sciences, USA* **93**: 2213–2218.

Tyystjärvi E, **Mäenpää P**, **Aro EM. 1994**. Mathematical modelling of photoinhibition and Photosystem II repair cycle. I. Photoinhibition and D1 protein degradation *in vitro* and in the absence of chloroplast protein synthesis *in vivo*. *Photosynthesis Research* **41**: 439–449.

Tyystjärvi T, **Tuominen I**, **Herranen M**, **Aro EM**, **Tyystjarvi E. 2002**. Action spectrum of psbA gene transcription is similar to that of photoinhibition in *Synechocystis* sp. PCC 6803. *FEBS Letters* **516**: 167–171.

Vass I. 2011. Role of charge recombination processes in photodamage and photoprotection of the photosystem II complex. *Physiologia Plantarum* **142**: 6–16.

Watanabe M. 1995. Action spectroscopy: photomovement and photomorphogenesis spectra. In: Horsepool WM, Song P-S. *CRC handbook of organic photochemistry and photobiology*. Boca Raton, FL: CRC Press, 1276–1288.

Watanabe M, **Furuya M**, **Miyoshi Y**, **Inoue Y**, **Iwahashi I**, **Matsumoto K. 1982**. Design and performance of the OKAZAKI large spectrograph for photobiological research. *Photochemistry and Photobiology* **36**: 491–498.

Wünschmann G, **Brand JJ. 1992**. Rapid turnover of a component required for photosynthesis explains temperature dependence and kinetics of photoinhibition in a cyanobacterium, *Synechococcus* 6301. *Planta* **186**: 426–433.

Xiong F. 2001. Evidence that UV-B tolerance of the photosynthetic apparatus in microalgae is related to the D1-turnover mediated repair cycle *in vivo*. *Journal of Plant Physiology* **158**: 285–294.

Xiong FS, **Day TA. 2001**. Effect of solar ultraviolet-B radiation during springtime ozone depletion on photosynthesis and biomass production of Antarctic vascular plants. *Plant Physiology* **125**: 738–751.

Yamamoto Y, **Akasaka T. 1995**. Degradation of antenna chlorophyll-binding protein CP43 during photoinhibition of photosystem II. *Biochemistry* **34**: 9038–9045.

Zavafer A, **Cheah MH**, **Hillier W**, **Chow WS**, **Takahashi S. 2015**. Photodamage to the oxygen evolving complex of photosystem II by visible light. *Scientific Reports* **5**: 16363.

Zhan GM, **Li RJ**, **Hu ZY**, ***et al.*** **2014**. Cosuppression of *RBCS3B* in *Arabidopsis* leads to severe photoinhibition caused by ROS accumulation. *Plant Cell Reports* **33**: 1091–1108

Zhang Z, **Jia Y**, **Gao H**, **Zhang L**, **Li H**, **Meng Q. 2011**. Characterization of PSI recovery after chilling-induced photoinhibition in cucumber (*Cucumis sativus* L.) leaves. *Planta* **234**: 883–889

Zulfugarov IS, **Tovuu A**, **Eu YJ**, ***et al.*** **2014**. Production of superoxide from Photosystem II in a rice (*Oryza sativa* L.) mutant lacking PsbS. *BMC Plant Biology* **14**: 242.